



TECH BRIEFS

NATIONAL AERONAUTICS AND SPACE ADMINISTRATION

-  **Technology Focus**
-  **Computers/Electronics**
-  **Software**
-  **Materials**
-  **Mechanics**
-  **Machinery/Automation**
-  **Manufacturing**
-  **Bio-Medical**
-  **Physical Sciences**
-  **Information Sciences**
-  **Books and Reports**

INTRODUCTION

Tech Briefs are short announcements of innovations originating from research and development activities of the National Aeronautics and Space Administration. They emphasize information considered likely to be transferable across industrial, regional, or disciplinary lines and are issued to encourage commercial application.

Availability of NASA Tech Briefs and TSPs

Requests for individual Tech Briefs or for Technical Support Packages (TSPs) announced herein should be addressed to

National Technology Transfer Center

Telephone No. (800) 678-6882 or via World Wide Web at www2.nttc.edu/leads/

Please reference the control numbers appearing at the end of each Tech Brief. Information on NASA's Commercial Technology Team, its documents, and services is also available at the same facility or on the World Wide Web at www.nctn.hq.nasa.gov.

Commercial Technology Offices and Patent Counsels are located at NASA field centers to provide technology-transfer access to industrial users. Inquiries can be made by contacting NASA field centers and program offices listed below.

NASA Field Centers and Program Offices

Ames Research Center

Carolina Blake
(650) 604-1754
cblake@mail.arc.nasa.gov

Dryden Flight Research Center

Jenny Baer-Riedhart
(661) 276-3689
jenny.baer-riedhart@dfrc.nasa.gov

Goddard Space Flight Center

Nona Cheeks
(301) 286-5810
Nona.K.Cheeks.1@gssc.nasa.gov

Jet Propulsion Laboratory

Art Murphy, Jr.
(818) 354-3480
arthur.j.murphy-jr@jpl.nasa.gov

Johnson Space Center

Charlene E. Gilbert
(281) 483-3809
commercialization@jsc.nasa.gov

Kennedy Space Center

Jim Aliberti
(321) 867-6224
Jim.Aliberti-1@ksc.nasa.gov

Langley Research Center

Sam Morello
(757) 864-6005
s.a.morello@larc.nasa.gov

John H. Glenn Research Center at Lewis Field

Larry Viterna
(216) 433-3484
cto@grc.nasa.gov

Marshall Space Flight Center

Vernotto McMillan
(256) 544-2615
vernotto.mcmillan@msfc.nasa.gov

Stennis Space Center

Robert Bruce
(228) 688-1929
robert.c.bruce@nasa.gov

NASA Program Offices

At NASA Headquarters there are seven major program offices that develop and oversee technology projects of potential interest to industry:

Carl Ray

Small Business Innovation Research Program (SBIR) & Small Business Technology Transfer Program (STTR)
(202) 358-4652 or
cray@mail.hq.nasa.gov

Dr. Robert Norwood

Office of Commercial Technology (Code RW)
(202) 358-2320 or
rnorwood@mail.hq.nasa.gov

John Mankins

Office of Space Flight (Code MP)
(202) 358-4659 or
jmankins@mail.hq.nasa.gov

Terry Hertz

Office of Aero-Space Technology (Code RS)
(202) 358-4636 or
thertz@mail.hq.nasa.gov

Glen Mucklow

Office of Space Sciences (Code SM)
(202) 358-2235 or
gmucklow@mail.hq.nasa.gov

Roger Crouch

Office of Microgravity Science Applications (Code U)
(202) 358-0689 or
rcrouch@hq.nasa.gov

Granville Paules

Office of Mission to Planet Earth (Code Y)
(202) 358-0706 or
gpaules@mtpe.hq.nasa.gov



TECH BRIEFS

NATIONAL AERONAUTICS AND SPACE ADMINISTRATION



5 Technology Focus: Test & Measurement

- 5 Nulling Infrared Radiometer for Measuring Temperature
- 6 The Ames Power Monitoring System
- 7 Hot Films on Ceramic Substrates for Measuring Skin Friction
- 8 Probe Without Moving Parts Measures Flow Angle
- 9 Detecting Conductive Liquid Leaking From Nonconductive Pipe



11 Computers/Electronics

- 11 Adaptive Suppression of Noise in Voice Communications
- 12 High-Performance Solid-State W-Band Power Amplifiers
- 12 Microbatteries for Combinatorial Studies of Conventional Lithium-Ion Batteries
- 13 Correcting for Beam Aberrations in a Beam-Waveguide Antenna
- 14 Advanced Rainbow Solar Photovoltaic Arrays
- 15 Metal Side Reflectors for Trapping Light in QWIPs



17 Software

- 17 Software for Collaborative Engineering of Launch Rockets
- 17 Software Assists in Extensive Environmental Auditing
- 17 Software Supports Distributed Operations via the Internet
- 17 Software Estimates Costs of Testing Rocket Engines
- 18 yourSky: Custom Sky-Image Mosaics via the Internet
- 18 Software for Managing Inventory of Flight Hardware



19 Materials

- 19 Lower-Conductivity Thermal-Barrier Coatings
- 19 Process for Smoothing an Si Substrate After Etching of SiO₂
- 20 Flexible Composite-Material Pressure Vessel
- 20 Treatment To Destroy Chlorohydrocarbon Liquids in the Ground



23 Mechanics

- 23 Noncircular Cross Sections Could Enhance Mixing in Sprays



25 Machinery/Automation

- 25 Small, Untethered, Mobile Robots for Inspecting Gas Pipes



27 Manufacturing

- 27 Paint-Overspray Catcher
- 27 Preparation of Regular Specimens for Atom Probes
- 28 Inverse Tomo-Lithography for Making Microscopic 3D Parts



31 Physical Sciences

- 31 Predicting and Preventing Incipient Flameout in Combustors
- 32 MEMS-Based Piezoelectric/Electrostatic Inchworm Actuator
- 32 Metallized Capillaries as Probes for Raman Spectroscopy



35 Information Sciences

- 35 Adaptation of Mesoscale Weather Models to Local Forecasting
- 35 Aerodynamic Design Using Neural Networks
- 36 Combining Multiple Gyroscope Outputs for Increased Accuracy
- 38 Improved Collision-Detection Method for Robotic Manipulator

This document was prepared under the sponsorship of the National Aeronautics and Space Administration. Neither the United States Government nor any person acting on behalf of the United States Government assumes any liability resulting from the use of the information contained in this document, or warrants that such use will be free from privately owned rights.



Nulling Infrared Radiometer for Measuring Temperature

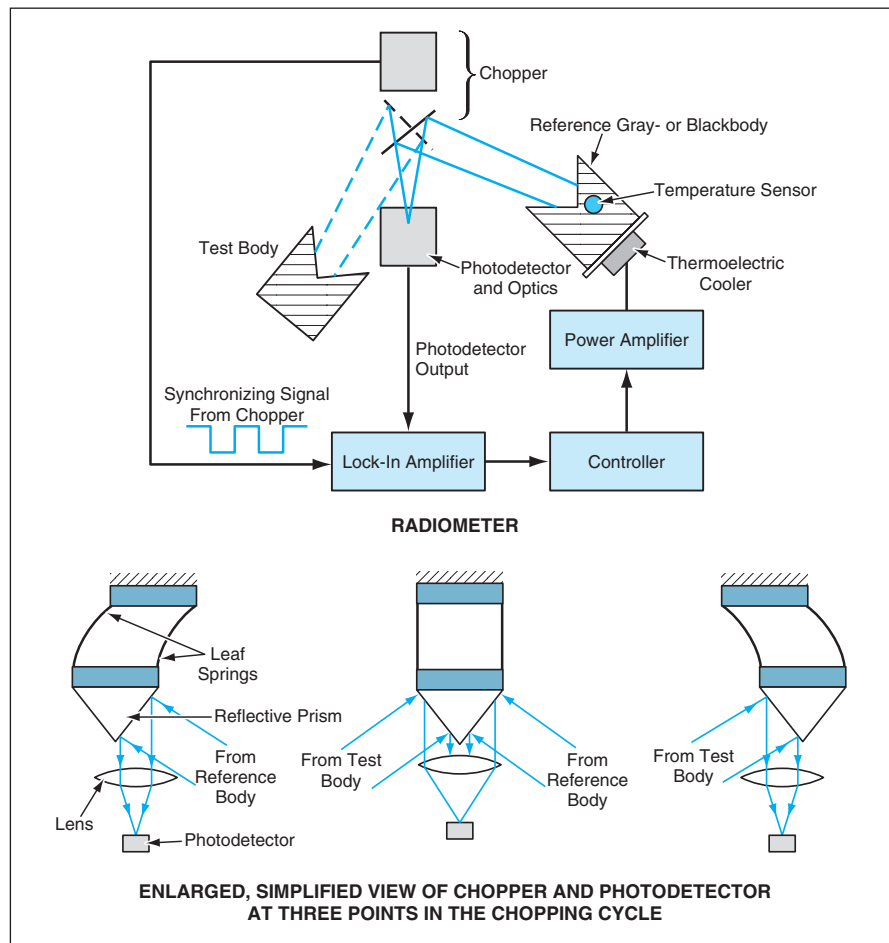
A microwave-radiometer self-calibration principle would be adapted to measurement of infrared.

Stennis Space Center, Mississippi

A nulling, self-calibrating infrared radiometer is being developed for use in noncontact measurement of temperature in any of a variety of industrial and scientific applications. This instrument is expected to be especially well-suited to measurement of ambient or near-ambient temperature and, even more specifically, for measuring the surface temperature of a natural body of water. Although this radiometer would utilize the long-wavelength infrared (LWIR) portion of the spectrum (wavelengths of 8 to 12 μm), its basic principle of operation could also be applied to other spectral bands (corresponding to other temperature ranges) in which the atmosphere is transparent and in which design requirements for sensitivity and temperature-measurement accuracy could be satisfied.

The underlying principle of nulling and self-calibration is the same as that of a typical microwave radiometer, but because of differences between the characteristics of signals in the infrared and microwave spectral regions, the principle must be implemented in a different way. The instrument (see figure) would include an infrared photodetector equipped with focusing input optics [e.g., lens(es) and/or mirrors] and an input LWIR band-pass filter. An optomechanical device would periodically chop the input to the photodetector between a reference gray body (ideally, a blackbody) and a test body (the temperature of which one seeks to measure). The reference body would be mounted on or in a heater, a thermoelectric cooler, or other temperature-control device suited to the particular application. If needed, a band-pass LWIR filter could be placed in front of the photodetector.

The AC component of the photodetector output would be fed to a lock-in amplifier. The reference or synchronization signal for the lock-in amplifier would be derived from a device that monitored the motion of the chopper. The output of the lock-in amplifier would be a rectified signal approximately proportional to the difference between the radiances of the test body and the reference body. This signal would be used as an error signal in a feed-



This Infrared Radiometer would exploit a nulling, self-calibrating principle that, heretofore, has been the basis of design and operation of many microwave radiometers. The leaf-spring resonator design of the chopper would be an important element of the overall design of the instrument.

back control loop, which would adjust the power supplied to the temperature-control device and thereby adjust the temperature of the reference body in an effort to reduce the error to zero. The temperature of the reference body would be measured by any of a variety of commercially available contact temperature sensors, which can routinely afford accuracy and long-term stability within 0.1 K. Hence, as long as the error voltage remained at zero and assuming that the emissivities and other radiant properties of the test and reference bodies were sufficiently similar, it could be assumed that the measured reference-body temperature was a close ap-

proximation of the test-body temperature.

Initial development efforts have been concentrated on the chopper, which is a major innovative feature of the instrument design. The desired characteristics of the chopper include pure chopping, low power consumption (a few milliwatts), high reliability (millions of cycles), and a chopping frequency of several hertz. "Pure chopping" signifies that at any given instant of time, the infrared radiation incident on the photodetector would be that from the test body and/or the reference body and not from the chopper itself and that, moreover, during one designated portion of the chopping

cycle, the photodetector would “see” only the test body while during another designated portion of the cycle it would “see” only the reference body.

The chopper design under consideration at the time of reporting the information for this article calls for an electro-mechanical resonator comprising two permanent magnets and a reflective

prism mounted on leaf springs. Each permanent magnet would interact with one of two electromagnet coils. One electromagnet coil would be driven by amplifier to excite vibrations. The other electromagnet coil would serve as a pickup coil, providing feedback to the amplifier to set up oscillations at the mechanical resonance frequency.

This work was done by Robert Ryan of Lockheed Martin Corp. for Stennis Space Center.

This invention is owned by NASA, and a patent application has been filed. Inquiries concerning nonexclusive or exclusive license for its commercial development should be addressed to the Intellectual Property Manager, Stennis Space Center; (228) 688-1929. Refer to SSC-00124.

The Ames Power Monitoring System

Power demand can be managed to reduce cost.

Ames Research Center, Moffett Field, California

The Ames Power Monitoring System (APMS) is a centralized system of power meters, computer hardware, and special-purpose software that collects and stores electrical power data by various facilities at Ames Research Center (ARC). This system is needed because of the large and varying nature of the overall ARC power demand, which has been observed to range from 20 to 200 MW. Large portions of peak demand can be attributed to only three wind tunnels (60, 180, and 100 MW, respectively). The APMS helps ARC avoid or minimize costly demand charges by enabling wind-tunnel operators, test engineers, and the power manager to monitor total demand for center in real time. These persons receive the information they need to manage and schedule energy-intensive research in advance and to adjust loads in real time to ensure that the overall maximum allowable demand is not exceeded.

The APMS (see figure) includes a server computer running the Windows NT operating system and can, in principle, include an unlimited number of power meters and client computers. As configured at the time of reporting the information for this article, the APMS includes more than 40 power meters monitoring all the major research facilities, plus 15 Windows-based client personal computers that display real-time and historical data to users via graphical user interfaces (GUIs). The power meters and client computers communicate with the server using Transmission Control Protocol/Internet Protocol (TCP/IP) on Ethernet networks, variously, through dedicated fiber-optic cables or through the pre-existing ARC local-area network (ARCLAN).

The APMS has enabled ARC to achieve significant savings (\$1.2 million in 2001) in the cost of power and

electric energy by helping personnel to maintain total demand below monthly allowable levels, to manage the overall power factor to avoid low power factor penalties, and to use historical system data to identify opportunities for additional energy savings. The APMS also provides power engineers and electricians with the information they need to plan modifications in advance and perform day-to-day maintenance of the ARC electric-power distribution system.

This work was done by Leonid Osetinsky of Jacobs/Sverdrup Technology and David Wong of Ames Research Center. For further information, please contact:

Leonid Osetinsky, P.E.

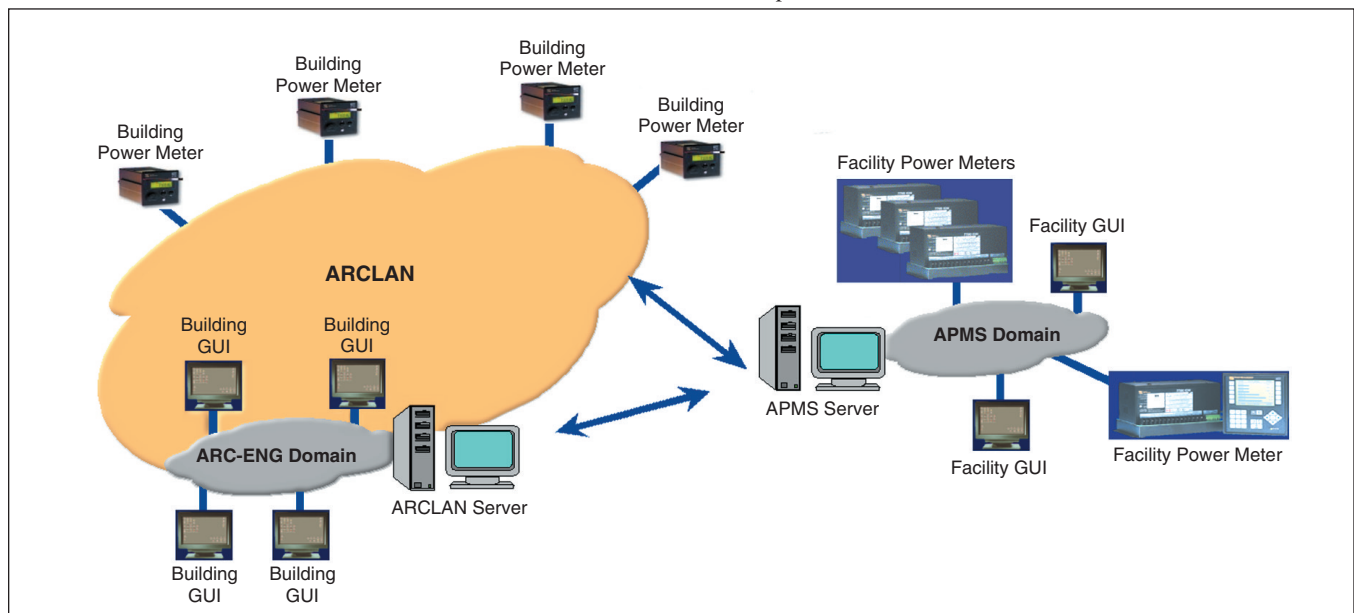
Jacobs/Sverdrup, Ames R&D Group

NASA Ames Research Center

Tel. No.: (650)604-2396

E-mail: losetinsky@mail.arc.nasa.gov

ARC-14909



The APMS collects, stores, and displays data on the consumption of electric power in major subsystems of the ARC power-distribution system.

Hot Films on Ceramic Substrates for Measuring Skin Friction

Low-thermal-conductivity ceramic substrates, based on Space Shuttle tile technology, serve to increase sensitivity.

Dryden Flight Research Center, Edwards, California

Hot-film sensors, consisting of a metallic film on an electrically nonconductive substrate, have been used to measure skin friction as far back as 1931. A hot film is maintained at an elevated temperature relative to the local flow by passing an electrical current through it. The power required to maintain the specified temperature depends on the rate at which heat is transferred to the flow. The heat-

transfer rate correlates to the velocity gradient at the surface, and hence, with skin friction. The hot-film skin friction measurement method is most thoroughly developed for steady-state conditions, but additional issues arise under transient conditions.

Fabricating hot-film substrates using low-thermal-conductivity ceramics can offer advantages over traditional quartz or

polyester-film substrates. First, a low conductivity substrate increases the fraction of heat convected away by the fluid, thus increasing sensitivity to changes in flow conditions. Furthermore, the two-part, composite nature of the substrate allows the installation of thermocouple junctions just below the hot film, which can provide an estimate of the conduction heat loss.

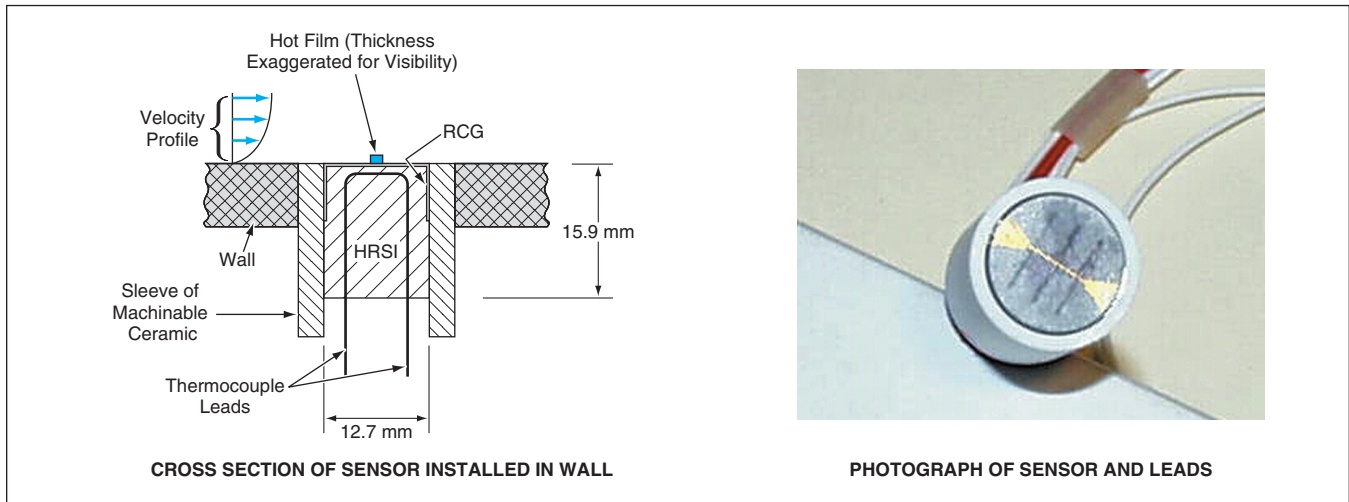


Figure 1. The Composite Ceramic Substrate of this hot-film sensor reduces conduction losses and increases sensitivity.

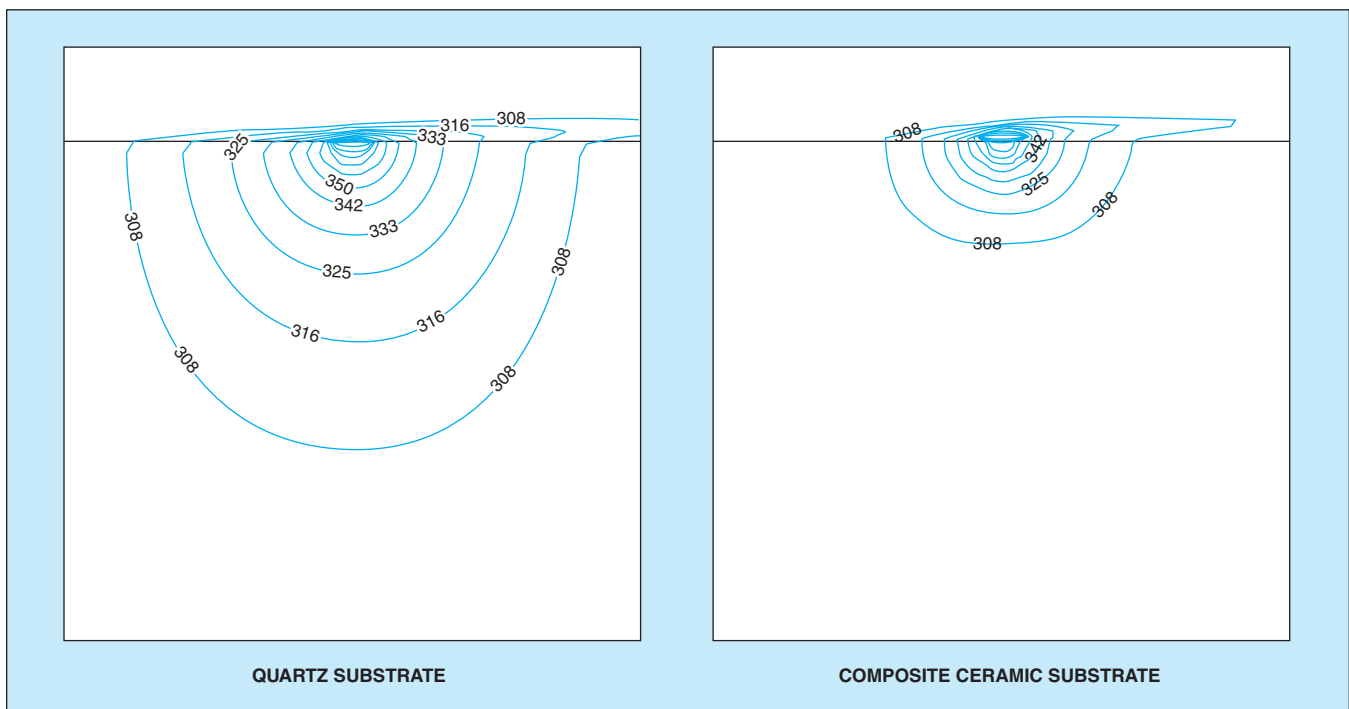


Figure 2. Steady-State Temperature Contours, determined from conjugate heat-transfer analyses, illustrate the effect of the lower thermal conductivity of the composite ceramic substrate relative to a quartz substrate. Temperatures are indicated in °C.

Figure 1 depicts a hot-film sensor of this type. The substrate is primarily composed of high-temperature reusable shuttle insulation (HRSI), a lightweight (density = 352 kg/m³), porous, ceramic material originally developed to protect the space shuttle from aerodynamic heating. A hard, non-porous coat of reaction-cured glass (RCG) extends over the face of the cylinder and about one-third of the way down the side providing a surface on which the metallic hot film and its leads can be deposited. Small-diameter [0.005 in. (0.127 mm)] thermocouple wires are routed through the HRSI. Small grooves in the end of the HRSI cylinder, form the lands of the thermocouples and are deep enough such that the wires lie flush with the HRSI surface prior to being coated with the RCG. The three thermocouple junctions are placed in a line. The substrates are placed in a machinable-cer-

amic sleeve that provides electrical isolation for the hot-film leads. Type R thermocouples must be used because the high firing temperature of the RCG coating precludes the use of the more-sensitive thermocouples of type K's.

The hot film itself is approximately 0.004 in. (≈ 0.102 mm) wide and 1/4 in. (6.35 mm) long. Fabrication of the hot film and its leads begins with hand painting the desired pattern using organo-metallic inks. The painted substrate is then heated in an oven, which removes the solvents from the ink leaving only a gold-alloy film (see Figure 1 photo). The sensor thermocouples provide feedback control to the oven. These techniques could be used for the fabrication of other temperature and heat-flux gauges on high-temperature ceramics.

Conjugate heat-transfer analyses were performed on different substrate mate-

rials in air at moderate velocity gradients (7,500 s⁻¹). For the composite ceramic substrate, the ratio of heat leaving the sensor via convection to total heat produced is about 4 times higher than for a quartz substrate. Figure 2 depicts steady-state temperature contours for quartz and a composite ceramic substrate. Preliminary bench tests comparing hot films on composite ceramic and machinable-ceramic substrates indicate that, at overheat ratios of 1.2 and in horizontal orientations, the higher conductivity machinable-ceramic substrates require over 2.5 times the power.

This work was done by Greg Noffz of Dryden Flight Research Center, Daniel Leiser of Ames Research Center, Jim Bartlett of Langley Research Center, and Adrienne Lavine of UCLA. For further information, contact the Dryden Commercial Technology Office at (661) 276-3689. DRC-01-48

Probe Without Moving Parts Measures Flow Angle

Flow angle is computed from forces measured by use of strain gauges.

Dryden Flight Research Center, Edwards, California

The measurement of local flow angle is critical in many fluid-dynamic applications, including the aerodynamic flight testing of new aircraft and flight systems. Flight researchers at NASA Dryden Flight Research Center have recently developed, flight-tested, and patented the force-based flow-angle probe (FLAP), a novel, force-based instrument for the measurement of local flow direction. Containing no moving parts, the FLAP may provide greater simplicity, improved accuracy, and increased measurement access, relative to conventional moving-vane-type flow-angle probes.

Forces in the FLAP can be measured by various techniques, including those that involve conventional strain gauges (based on electrical resistance) and those that involve more advanced strain gauges (based on optical fibers). A correlation is used to convert force-measurement data to the local flow angle. The use of fiber optics will enable the construction of a miniature FLAP, leading to the possibility of flow measurement in very small or confined regions. This may also enable the "tufting" of a surface with miniature FLAPs, capable of quantitative flow-angle measurements, similar to attaching yarn tufts for qualitative measurements.

The prototype FLAP was a small, aerodynamically shaped, low-aspect-

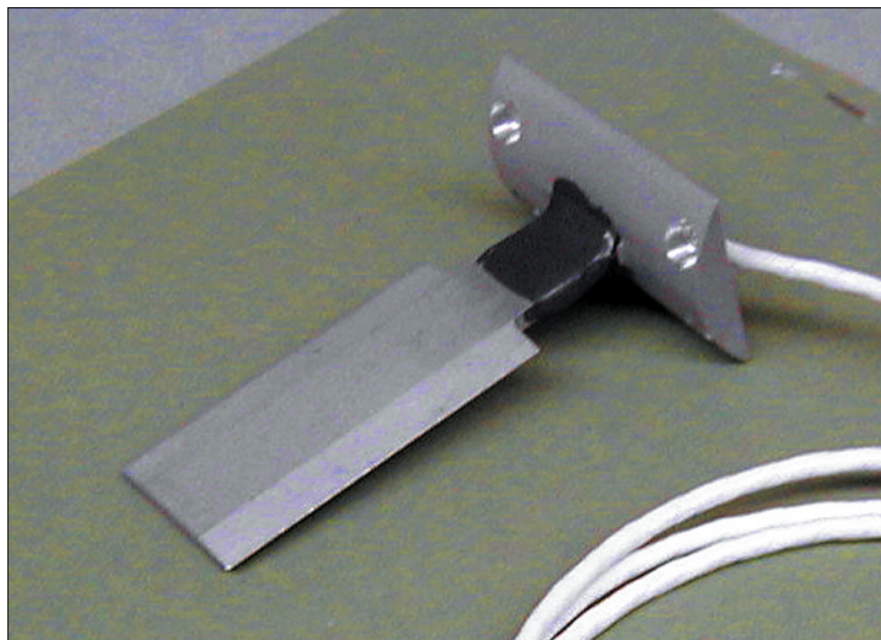


Figure 1. The **Prototype FLAP** was a fin instrumented with simple electrical-resistance strain gauges.

ratio fin about 2 in. (≈ 5 cm) long, 1 in. (≈ 2.5 cm) wide, and 0.125 in. (≈ 0.3 cm) thick (see Figure 1). The prototype FLAP included simple electrical-resistance strain gauges for measuring forces. Four strain gauges were mounted on the FLAP; two on the upper surface and two on the lower surface. The gauges were connected to

form a full Wheatstone bridge, configured as a bending bridge.

In preparation for a flight test, the prototype FLAP was mounted on the air-data boom of a flight-test fixture (FTF) on the NASA Dryden F-15B flight research airplane. The FTF is an aerodynamic fixture for flight-research experiments that is carried underneath the

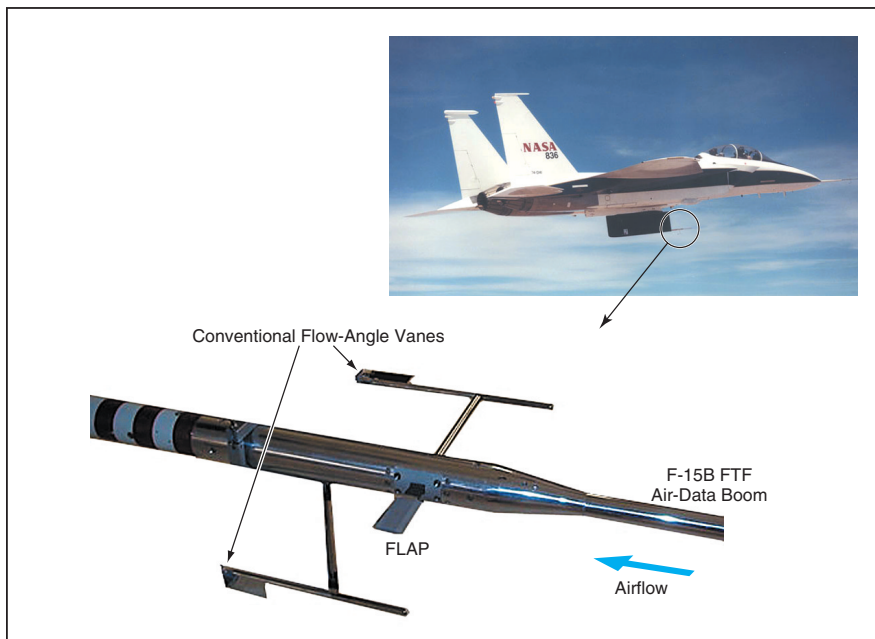


Figure 2. The Air-Data Boom of the F-15B FTF was used to carry the FLAP in a flight test.

F-15B fuselage (see Figure 2). Measurement data were collected as the FLAP was flown on the F-15B at subsonic and supersonic speeds up to mach 1.7 and altitudes up to 45,000 ft (≈ 13.7 km). FLAP data were also collected under high-angle-of-attack and high-vertical-acceleration flight conditions. The flight data analyzed to date have verified the feasibility of the FLAP concept.

In a second-generation FLAP now under development, the electrical-resistance-strain-gauge force-measurement system of the prototype FLAP is replaced with a fiber-optic-strain-gauge force-measurement system. This FLAP will also be flown on the NASA Dryden F-15B airplane.

This work was done by Stephen Corda and M. Jake Vachon of Dryden Flight Research Center. Inquiries concerning nonexclusive or exclusive license for its commercial development should be addressed to Dryden Flight Research Center, Commercial Technology Office, (661) 276-3689. Refer to DRC-01-09.

🌀 Detecting Conductive Liquid Leaking From Nonconductive Pipe

A capacitive detector is scanned over the ground above the pipe.

John F. Kennedy Space Center, Florida

A method that can be implemented with relatively simple electronic circuitry provides a capability for detecting leakage of an electrically conductive liquid from an electrically nonconductive underground pipe. Alternatively or in addition, the method can be applied to locate the pipe, whether or not there is a leak. Although the method is subject to limitations (some of which are described below), it is still attractive as an additional option for detecting leaks and locating pipes without need for extensive digging.

The method is based on capacitive coupling of an alternating electrical signal from the liquid to a portable electronic unit that resembles a metal detector. A signal voltage is applied to the liquid at some convenient point along the pipe: for example, the signal could be coupled into the liquid via an aboveground metal pipe fitting, the interior surface of which is in contact with the liquid. The signal is conducted through the liquid in the pipe; in the case of diffusive leak of liquid into the surrounding ground, the signal is conducted through the leak, into the portion of the adjacent ground that has

become soaked with the liquid. (A drip leak cannot be detected by this method because there is no conductive path between the liquid inside and the liquid outside the pipe.)

The portable unit includes an electrically conductive plate connected to the input terminal of an amplifier. When the plate is brought near the pipe or the leaked liquid, a small portion of the signal power is coupled capacitively from the liquid to the plate. The user scans the plate near the ground surface to find the locus of maximum signal strength. The leak can be identified as a relatively wide area, contiguous with the location of the pipe, over which the signal is detectable.

In order for this method to work, the liquid must be sufficiently conductive, and must be significantly more conductive than the ground is. Thus, for example, the method does not work for pure water, which is nonconductive, and does not work where the ground has been soaked by a source other than a leak (e.g., heavy rain). It should be possible to apply this method to, for example, common polyvinyl chloride (PVC) pipes that contain impure water

(e.g., swimming-pool water) leaking into fairly dry ground.

The resistance of a typical column of water in a PVC pipe is of the order of megohms. The combination of this order of magnitude of resistance with the order of magnitude of capacitance in a typical practical case dictates the use of a signal frequency or frequencies no higher than the low kilohertz range. Using the audibility of signals in the frequency range to make a virtue out of necessity, one could feed the detector-amplifier output to a set of earphones so that the user could keep visual attention focused on scanning the plate of the portable unit while listening for the signal.

This work was done by Robert C. Youngquist of Kennedy Space Center. Further information is contained in a TSP (see page 1).

Inquiries concerning rights for the commercial use of this invention should be addressed to the Technology Programs and Commercialization Office, Kennedy Space Center, (321) 867-8130. Refer to KSC-12255.



Adaptive Suppression of Noise in Voice Communications

A digital signal processor effects SNR-dependent spectral subtraction.

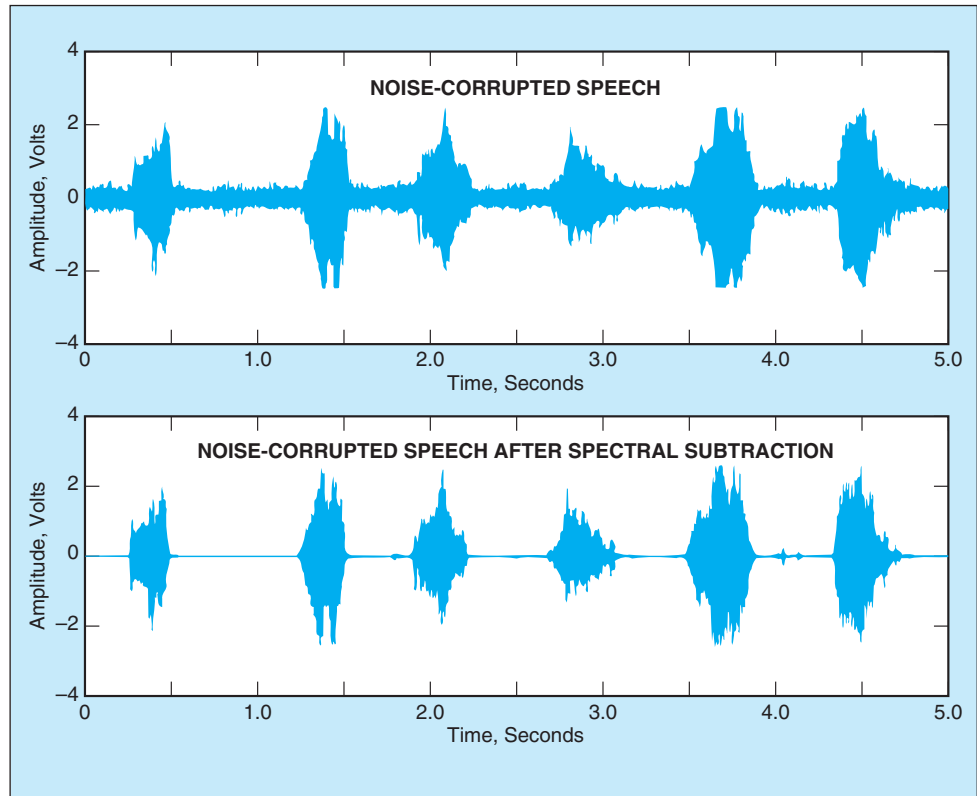
John F. Kennedy Space Center, Florida

A subsystem for the adaptive suppression of noise in a voice-communication system effects a high level of reduction of noise that enters the system through microphones. The subsystem includes a digital signal processor (DSP) plus circuitry that implements voice-recognition and spectral-manipulation techniques.

The development of the adaptive noise-suppression subsystem was prompted by the following considerations: During processing of the space shuttle at Kennedy Space Center, voice communications among test team members have been significantly impaired in several instances because some test participants have had to communicate from locations with high ambient noise levels. Ear protection for the personnel involved is commercially available and is used in such situations. However, commercially available noise-canceling microphones do not provide sufficient reduction of noise that enters through microphones and thus becomes transmitted on out-bound communication links.

In operation, noise or noise-corrupted speech enters the adaptive noise-suppression subsystem through a microphone. The output of the microphone is sent through a high-gain amplifier and an antialiasing low-pass filter. The output of the filter is sampled by an analog-to-digital converter.

At this point, the DSP suppresses noise by executing a spectral-subtraction algorithm that incorporates a dependence on the signal-to-noise ratio (SNR). The noise level and the SNR for use in the algorithm are determined by a subalgorithm that includes the following steps: First, each frame of raw data put out by the analog-to-digital converter is examined to determine whether it is a voiced or an unvoiced frame. An estimate of the noise is obtained during each unvoiced frame. A running average of the noise is then



The Noise in a Noisy Speech Signal was reduced nearly to zero by the spectral-subtraction process.

computed and used to approximate the expected value of the noise.

Using the SNR computed as described above, the SNR-dependent algorithm pre-emphasizes the frequency components of the input signal that contain the consonant information in human speech. The algorithm then determines the SNR and adjusts the proportion of spectral subtraction accordingly. After spectral subtraction, de-emphasis filtering is performed and low-amplitude signals are squelched. The resulting digital signal is processed through a digital-to-analog converter, then through a smoothing/voice-band filter, which is a band-pass filter with low and high 3-dB roll-off frequencies of 300 Hz and 3 kHz, respectively. The resulting analog signal is used to modulate a transmitter in the communication system.

In a demonstration of the adaptive noise-suppression system, the words

“test, one, two, three, four, five” were spoken into the microphone. The figure contains graphs of the original sampled noise-corrupted speech signal and the signal after spectral subtraction. Spectral subtraction increased the SNR by approximately 20 dB. A listening test verified that the original noise was virtually eliminated, and that little or no distortion in the form of musical noise was introduced.

This work was done by David Kozel of Purdue University, James A. DeVault of Kennedy Space Center, and Richard B. Birr formerly of I-NET, Inc. Further information is contained in a TSP (see page 1).

This invention is owned by NASA, and a patent application has been filed. Inquiries concerning nonexclusive or exclusive license for its commercial development should be addressed to the Technology Programs and Commercialization Office, Kennedy Space Center, (321) 867-6373. Refer to KSC-11937.

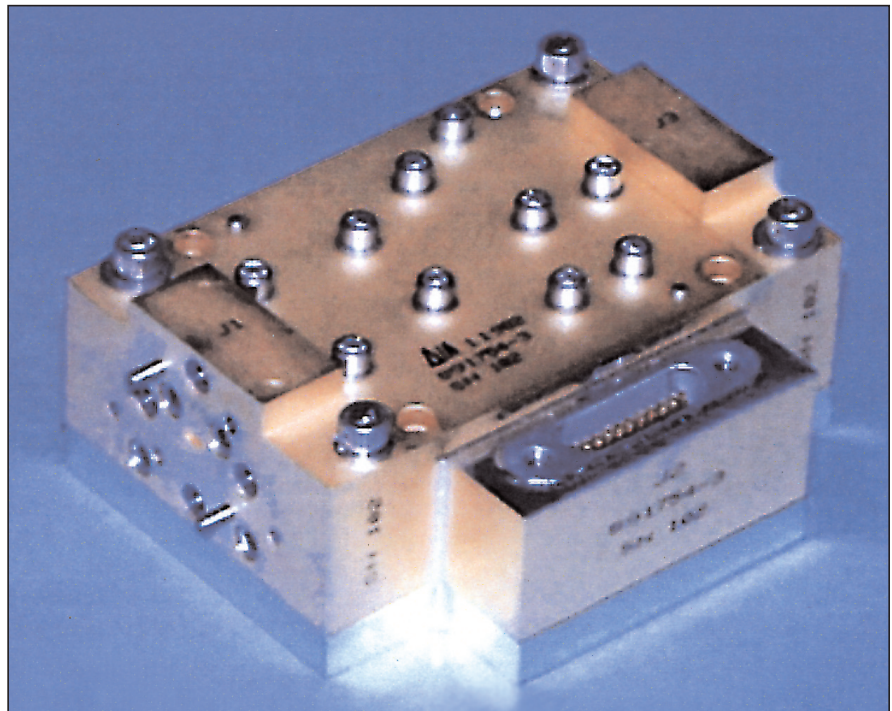
High-Performance Solid-State W-Band Power Amplifiers

Outputs ≥ 240 mW are available at frequencies from 71 to 106 GHz.

NASA's Jet Propulsion Laboratory, Pasadena, California

The figure shows one of four solid-state power amplifiers, each capable of generating an output power ≥ 240 mW over one of four overlapping frequency bands from 71 to 106 GHz. (The bands are 71 to 84, 80 to 92, 88 to 99, and 89 to 106 GHz.) The amplifiers are designed for optimum performance at a temperature of 130 K. These amplifiers were developed specifically for incorporation into frequency-multiplier chains in local oscillators in a low-noise, far-infrared receiving instrument to be launched into outer space to make astrophysical observations. The designs of these amplifiers may also be of interest to designers and manufacturers of terrestrial W-band communication and radar systems.

Each amplifier includes a set of six high-electron-mobility transistor (HEMT) GaAs monolithic microwave integrated-circuit (MMIC) chips, microstrip cavities, and other components packaged in a housing made from A-40 silicon-aluminum alloy. This alloy was chosen because, for the original intended spacecraft application, it offers an acceptable compromise among the partially competing requirements for high thermal conductivity, low mass, and low thermal expansion. Problems that were solved in designing the amplifiers included designing connectors and packages to fit the available space; designing microstrip signal-power splitters and combiners; matching of impedances across the frequency bands;



This photograph shows one of the amplifiers described in the text. A WR-10 waveguide input port is on the left end. The output port is on the right end, facing away. DC input and sensing conductors enter the package via a 21-pin connector. (Module dimensions: 20 × 49 × 60 mm.)

matching of the electrical characteristics of those chips installed in parallel power-combining arms; control and levelling of output power across the bands; and designing the MMICs, microstrips, and microstrip cavities to suppress tendencies toward oscillation in several modes, both inside and outside the desired frequency bands.

This work was done by Todd Gaier, Lorene Samoska, Mary Wells, Robert Ferber, John Pearson, April Campbell, and Alejandro Peralta of Caltech for NASA's Jet Propulsion Laboratory and Gerald Swift, Paul Yocum, and Yun Chung of TRW, Inc. Further information is contained in a TSP (see page 1). NPO-30724

Microbatteries for Combinatorial Studies of Conventional Lithium-Ion Batteries

Thousands of combinations of battery materials can be evaluated economically.

NASA's Jet Propulsion Laboratory, Pasadena, California

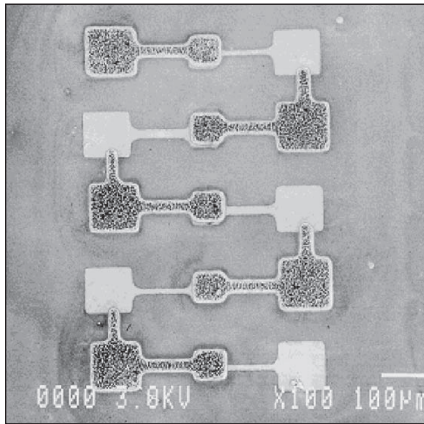
Integrated arrays of microscopic solid-state batteries have been demonstrated in a continuing effort to develop microscopic sources of power and of voltage reference circuits to be incorporated into low-power integrated circuits. Perhaps even more importantly, arrays of microscopic batteries can be fabricated and tested in combinatorial experiments

directed toward optimization and discovery of battery materials.

The value of the combinatorial approach to optimization and discovery has been proven in the optoelectronic, pharmaceutical, and bioengineering industries. Depending on the specific application, the combinatorial approach can involve the investigation of hundreds or

even thousands of different combinations; hence, it is time-consuming and expensive to attempt to implement the combinatorial approach by building and testing full-size, discrete cells and batteries. The conception of microbattery arrays makes it practical to bring the advantages of the combinatorial approach to the development of batteries.

Microbattery arrays (see figure) are fabricated on substrates by use of conventional integrated-circuit manufacturing techniques, including sputtering, photolithography, and plasma etching. The microbatteries incorporate the same cathode materials of interest for conventional lithium-ion batteries such as LiCoO_2 and $\text{LiCo}_x\text{Ni}_{1-x}\text{O}_2$. If multiple deposition sources are used in the fabrication of a given array, then the chemical compositions of battery components of interest can be varied across the substrate, making it possible to examine what amounts to almost a continuum of compositions. For example, assuming



This is a Scanning Electron Micrograph of a microbattery array. The lightly shaded contact pads are cathode current collectors. The darker contact pads are anode current collectors. The cathodes and solid electrolyte of each cell are sandwiched between the anode and cathode contact pads and are not visible in this view.

that a 4-in. (10-cm) substrate is used, the test-device pitch is $50\ \mu\text{m}$, and the concentration gradient is 80 percent across the substrate, then the compositions of adjacent test cells can be expected to differ by only about 0.04 percent. Because thousands of test cells can be fabricated in a single batch, it becomes practical to test thousands of combinations of battery materials by use of microbattery arrays, as contrasted with only about 10 to 20 combinations by use of macroscopic cells.

The following is an example of a procedure for fabricating an array of [$\text{LiCo}_x\text{Ni}_{1-x}\text{O}_2$ cathode/lithium phosphorus oxynitride solid electrolyte/nickel anode] cells like those shown in the figure, with a gradient in the cathode composition.

1. A Ti film is deposited on a 4-in. (≈ 10 -cm) oxidized Si substrate. A Mo film is subsequently deposited on the Ti film.
2. The Mo-Ti bilayer is patterned by use of photolithography and wet etching to define the cathode current collectors.
3. The substrate is patterned with thick negative photoresist, with vias in the photoresist opened over selected areas of the current collectors.
4. A film of $\text{LiCo}_x\text{Ni}_{1-x}\text{O}_2$ cathode material is deposited on the substrate with the desired gradient in x and selectively removed by use of a lift-off process, such that $\text{LiCo}_x\text{Ni}_{1-x}\text{O}_2$ is present only on the cathode current collectors.

5. A film of the solid electrolyte lithium phosphorous oxynitride is deposited.
6. A film of Ni is deposited.
7. The Ni film is patterned to define the anode current collectors.
8. The Ni film is selectively removed by ion milling.
9. A protective coat (for example, vapor-deposited Parylene) is applied.

All depositions described above are performed by magnetron sputtering. The procedure can be readily modified to yield gradients in the cathode with other cations of interest: for example, $\text{LiCo}_x\text{Ni}_{1-x}\text{O}_2$ could be replaced with $\text{LiCo}_x\text{Ni}_y\text{Mn}_{1-x-y}\text{O}_2$ with the desired gradients in x and y .

The cells can be tested by use of a commercial semiconductor-parameter analyzer connected to the test cells via tungsten probe needles. By applying a current of the order of 5 nA to a cell from the cathode to the anode, the cell can be charged by oxidizing the cathode and reducing the Li at the anode. The charged cell can be discharged by reversing the polarity of the current. The cells can be tested in the same manner as that used to test conventional lithium-ion cells to obtain information on such characteristics as cycle life and charge/discharge capacities, all as a function of compositions of the cathode.

*This work was done by William West, Jay Whitacre, and Ratnakumar Bugga of Caltech for NASA's Jet Propulsion Laboratory. Further information is contained in a TSP (see page 1).
NPO-21216*

Correcting for Beam Aberrations in a Beam-Waveguide Antenna

The transmitting feed is moved to compensate for movement of the target.

NASA's Jet Propulsion Laboratory, Pasadena, California

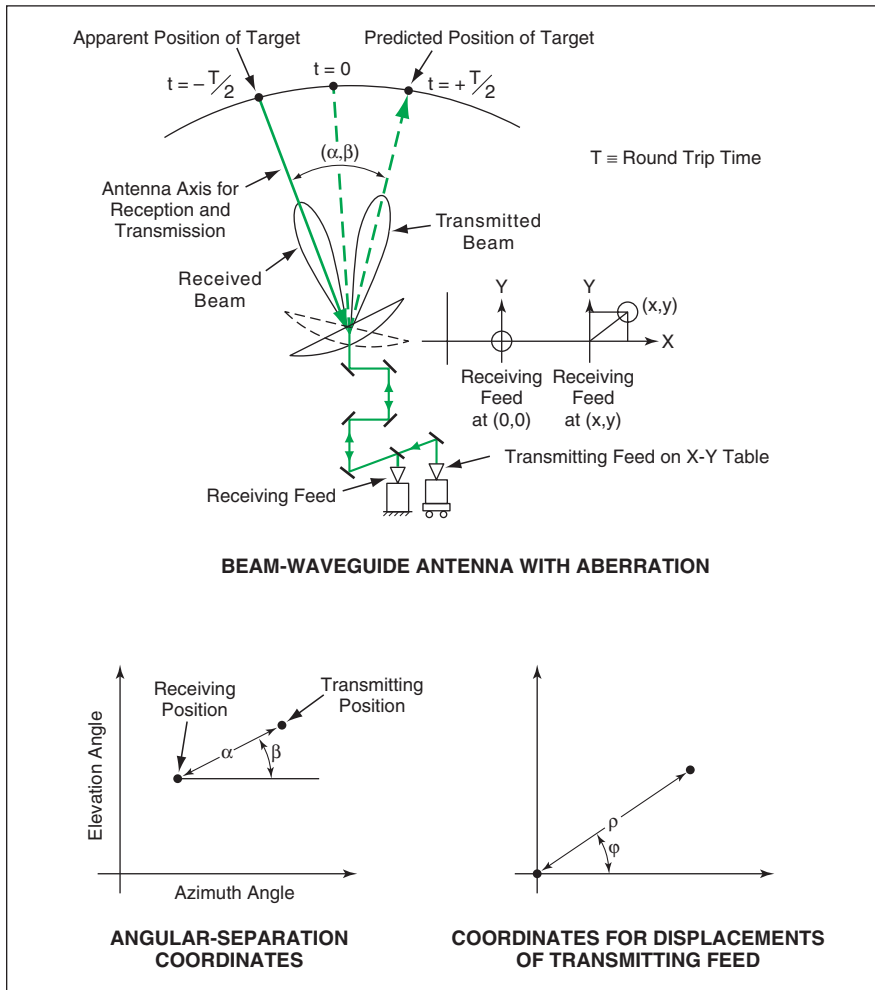
A method for correcting the aim of a beam-waveguide microwave antenna compensates for the beam aberration that occurs during radio tracking of a target that has a component of velocity transverse to the line of sight from the tracking station. The method was devised primarily for use in tracking of distant target spacecraft by large terrestrial beam-waveguide antennas of NASA's Deep Space Network (DSN). The method should also be adaptable to tracking, by other beam-waveguide antennas, of targets that move with large transverse velocities at large distances from the antennas.

The aberration effect arises whenever a spacecraft is not moving along

the line of sight as seen from an antenna on Earth. In such a case, the spacecraft has a cross-velocity component, which is normal to the line-of-sight direction. In order to obtain optimum two-way communication, the uplink and downlink beams must be pointed differently for simultaneous uplink and downlink communications. At any instant of time, the downlink (or receive, R_x) beam must be pointed at a position where the spacecraft was 1/2-round-trip light time (RTLTL) ago, and the uplink (or transmit, T_x) beam must be pointed where the spacecraft will be in 1/2 RTLTL (see figure). In the case of a high-

gain, narrow-beam antenna such as is used in the DSN, aiming the antenna in other than the correct transmitting or receiving direction, or aiming at a compromise direction between the correct transmitting and receiving directions, can give rise to several dB of pointing loss.

In the present method, the antenna is aimed directly at the apparent position of the target, so that no directional correction is necessary for reception of the signal from the target. Hence, the effort at correction is concentrated entirely on the transmitted beam. In physical terms, the correction is implemented by moving the transmitting feed along a small



The **Transmitting Feed Is Displaced in X and Y** by amounts needed to point the transmitting beam away from the receiving beam (which coincides with the antenna axis) by angular-separation amounts α and β .

displacement vector chosen so that the direction of the transmitted beam is altered by the small amount needed to make the beam point to the anticipated position of the target at the anticipated

time of arrival of the transmitted signal at the target.

The angular and linear coordinates mentioned in the following sentences are defined in the figure. The angular separation

between the transmitting and receiving beams is described in terms of the separation angle α and the clock angle β . The transmitting feed is mounted on an X-Y translation table. The problem is to compute the polar coordinates ρ and ϕ of the amount by which the transmitting feed must be displaced in the X-Y plane to move the direction transmitting beam, away from the direction of the receiving beam, by the amounts of the required angular separation. The problem becomes one of computing the ρ and ϕ needed to obtain the required α and β . (Then the required X and Y are calculated from ρ and ϕ by simple trigonometry.)

The algorithm used to control the X-Y table implements a closed-form representation of the coordinates ρ and ϕ as functions of the coordinates α and β . This representation can be obtained by experimentation and/or physical-optics-based, computational-simulation studies of electromagnetic scattering by the pertinent antenna optics configuration for various combinations of ρ and ϕ . The representation is of the general form

$$\rho = c_1\alpha + c_2\alpha^2 \text{ and}$$

$$\phi = \phi_F - \beta + \theta_{EL} - \theta_{AZ} - n\pi/2 \text{ radians,}$$

where c_1 and c_2 are coefficients determined by the computational study; ϕ_F is related to the feed position on the floor; θ_{EL} and θ_{AZ} are the elevation and azimuth angles, respectively; and n is one of the integers between -1 and $+2$, determined through measurements of beam offsets obtained at known feed offsets.

This work was done by Manuel Franco, Stephen Slobin, and Watt Veruttipong of Caltech for NASA's Jet Propulsion Laboratory. Further information is contained in a TSP (see page 1). NPO-30534

Advanced Rainbow Solar Photovoltaic Arrays

Concentrated sunlight is spectrally dispersed onto adjacent cells with different bandgaps.

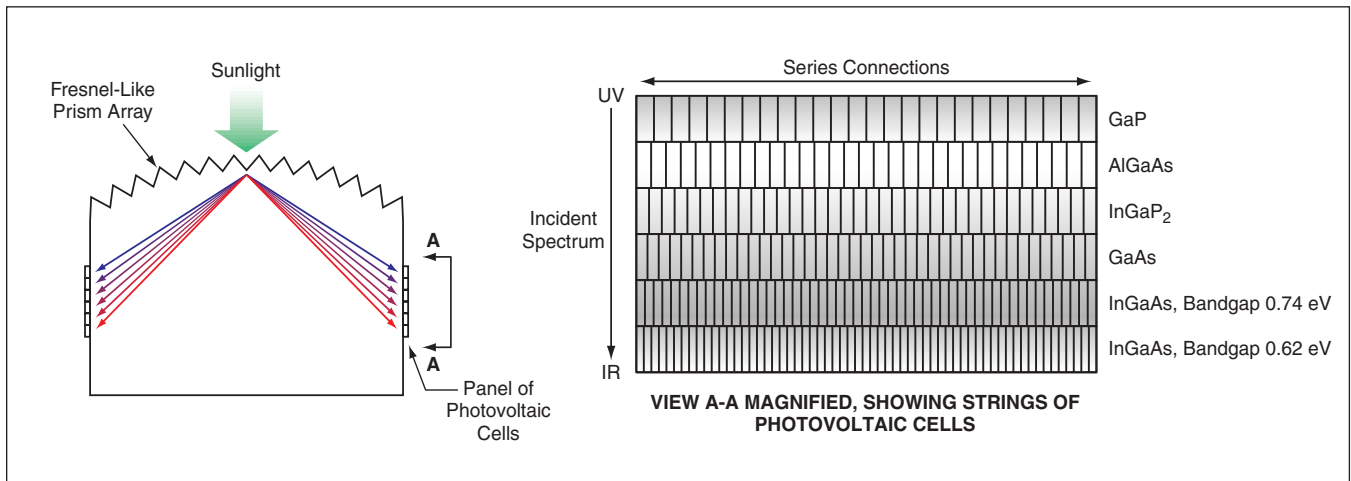
NASA's Jet Propulsion Laboratory, Pasadena, California

Photovoltaic arrays of the rainbow type, equipped with light-concentrator and spectral-beam-splitter optics, have been investigated in a continuing effort to develop lightweight, high-efficiency solar electric power sources. This investigation has contributed to a revival of the concept of the rainbow photovoltaic array, which originated in the 1950s but proved unrealistic at that time because the selection of solar photovoltaic cells was too limited. Advances in the art of photovoltaic cells

since that time have rendered the concept more realistic, thereby prompting the present development effort.

A rainbow photovoltaic array comprises side-by-side strings of series-connected photovoltaic cells. The cells in each string have the same bandgap, which differs from the bandgaps of the other strings. Hence, each string operates most efficiently in a unique wavelength band determined by its bandgap. To obtain maximum energy-conversion

efficiency and to minimize the size and weight of the array for a given sunlight-input aperture, the sunlight incident on the aperture is concentrated, then spectrally dispersed onto the photovoltaic-array plane, whereon each string of cells is positioned to intercept the light in its wavelength band of most efficient operation. The number of cells in each string is chosen so that the output potentials of all the strings are the same; this makes it possible to connect the



A **Curved Fresnel Prism** would concentrate and spectrally disperse sunlight onto adjacent strings of solar photovoltaic cells, each string optimized for the part of the spectrum incident upon it.

strings together in parallel to maximize the output current of the array.

According to the original rainbow photovoltaic concept, the concentrated sunlight was to be split into multiple beams by use of an array of dichroic filters designed so that each beam would contain light in one of the desired wavelength bands. The concept has since been modified to provide for dispersion of the spectrum by use of adjacent prisms. A proposal for an advanced version calls for a unitary concentrator/spectral-beam-splitter optic in the form of a parabolic curved Fresnel-like

prism array with panels of photovoltaic cells on two sides (see figure). The surface supporting the solar cells can be adjusted in length or angle to accommodate the incident spectral pattern.

An unoptimized prototype assembly containing ten adjacent prisms and three photovoltaic cells with different bandgaps (InGaP₂, GaAs, and InGaAs) was constructed to demonstrate feasibility. The actual array will consist of a lightweight thin-film silicon layer of prisms curved into a parabolic shape. In an initial test under illumination of 1 sun at

zero airmass, the energy-conversion efficiency of the assembly was found to be 20 percent. Further analysis of the data from this test led to a projected energy-conversion efficiency as high as 41 percent for an array of 6 cells or strings (GaP, AlGaAs, InGaP₂, GaAs, and two different InGaAs cells or strings).

This work was done by Nick Mardesich and Virgil Shields of Caltech for NASA's Jet Propulsion Laboratory. Further information is contained in a TSP (see page 1). NPO-21051

Metal Side Reflectors for Trapping Light in QWIPs

Quantum efficiency would be increased because light would make multiple passes.

NASA's Jet Propulsion Laboratory, Pasadena, California

Focal-plane arrays of quantum-well infrared photodetectors (QWIPs) equipped with both light-coupling diffraction gratings and metal side reflectors have been proposed, and prototypes are expected to be fabricated soon. The purpose served by the metal side reflectors is to increase quantum efficiency by helping to trap light in the photosensitive material of each pixel.

The reasons for using diffraction gratings were discussed in several prior NASA Tech Briefs articles. To recapitulate: In an array of QWIPs, the quantum-well layers are typically oriented parallel to the focal plane and therefore perpendicular or nearly perpendicular to the direction of incidence of infrared light. By virtue of the applicable quantum selection rules, light polarized parallel to the focal plane (as normally incident light is) cannot excite

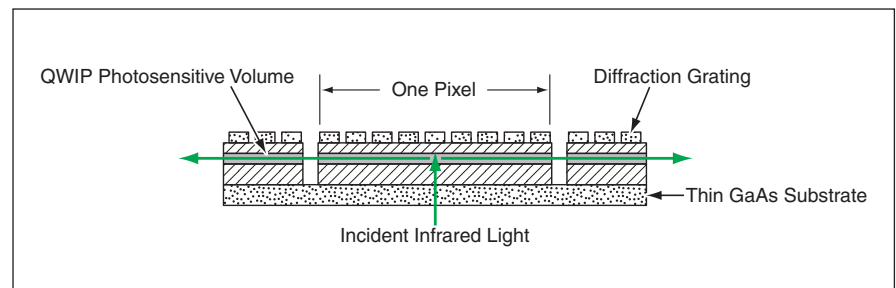


Figure 1. **Light Is Diffracted** almost parallel to the focal plane for maximum quantum efficiency in a QWIP of typical prior design. However, in the absence of reflectors like those shown in Figure 2, much of the diffracted light is lost from the QWIP of a given pixel after a single pass through the photosensitive QWIP volume.

charge carriers and, hence, cannot be detected. Diffraction gratings scatter normally or nearly normally incident light into directions more nearly parallel to the focal plane, so that a significant portion of the light attains a component of polarization normal to the focal plane and, hence, can

excite charge carriers. Unfortunately, light scattered in directions parallel or nearly parallel to the focal plane can escape sideways from the QWIP of a given pixel, as illustrated in Figure 1. The escaped light has made only a single pass through the interior photosensitive volume of the QWIP.

The quantum efficiency of the QWIP would be increased by trapping light so that it makes multiple passes through the photosensitive volume. As

shown in Figure 2, the sides of the QWIP of each pixel would be coated with gold to reflect escaping light back into the interior.

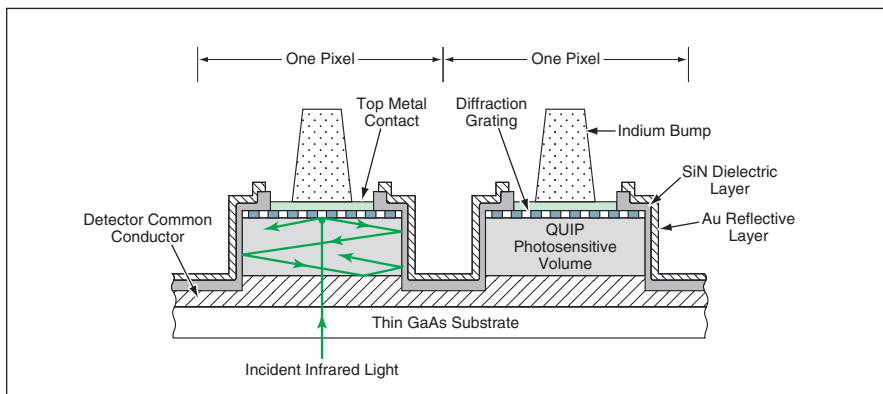


Figure 2. **Reflective Layers of Gold** in a QWIP array of the type now under development would make the light traverse the interior of each QWIP multiple times.

This work was done by Sarath Gunapala, Sumith Bandara, John Liu, and David Ting of Caltech for NASA's Jet Propulsion Laboratory. Further information is contained in a TSP (see page 1).

In accordance with Public Law 96-517, the contractor has elected to retain title to this invention. Inquiries concerning rights for its commercial use should be addressed to

Intellectual Assets Office

JPL

Mail Stop 202-233

4800 Oak Grove Drive

Pasadena, CA 91109

(818) 354-2240

E-mail: ipgroup@jpl.nasa.gov

Refer to NPO-30507, volume and number of this NASA Tech Briefs issue, and the page number.

Software for Collaborative Engineering of Launch Rockets

The **R**ocket **E**valuation and **C**ost **I**ntegration for **P**ropulsion and **E**ngineering software enables collaborative computing with automated exchange of information in the design and analysis of launch rockets and other complex systems. RECIPE can interact with and incorporate a variety of programs, including legacy codes, that model aspects of a system from the perspectives of different technological disciplines (e.g., aerodynamics, structures, propulsion, trajectory, aeroheating, controls, and operations) and that are used by different engineers on different computers running different operating systems. RECIPE consists mainly of (1) ISCRM — a file-transfer subprogram that makes it possible for legacy codes executed in their original operating systems on their original computers to exchange data and (2) CONES — an easy-to-use file-wrapper subprogram that enables the integration of legacy codes. RECIPE provides a tightly integrated conceptual framework that emphasizes connectivity among the programs used by the collaborators, linking these programs in a manner that provides some configuration control while facilitating collaborative engineering tradeoff studies, including “design to cost” studies. In comparison with prior collaborative-engineering schemes, one based on the use of RECIPE enables fewer engineers to do more in less time.

This program was written by Thomas Troy Stanley of International Space Systems, Inc., for Marshall Space Flight Center. Further information is contained in a TSP (see page 1). MFS-31692

Software Assists in Extensive Environmental Auditing

The Base Environmental Management System (BEMS) is a Web-based application program for managing and tracking audits by the Environmental Office of Stennis Space Center in conformity with standard 14001 of the International Organization for Standardization (ISO 14001). (This standard specifies requirements for an environmental-management system.) BEMS

saves time by partly automating what were previously manual processes for creating audit checklists; recording and tracking audit results; issuing, tracking, and implementing corrective-action requests (CARs); tracking continuous improvements (CIs); and tracking audit results and statistics. BEMS consists of an administration module and an auditor module. As its name suggests, the administration module is used to administer the audit. It helps administrators to edit the list of audit questions; edit the list of audit locations; assign mandatory questions to locations; track, approve, and edit CARs; and edit completed audits. The auditor module is used by auditors to perform audits and record audit results: it helps the auditors to create audit checklists, complete audits, view completed audits, create CARs, record and acknowledge CIs, and generate reports from audit results.

This program was written by Christopher Callac and Charlie Matherne of Lockheed Martin Corp. for Stennis Space Center.

Inquiries concerning rights for the commercial use of this invention should be addressed to the Intellectual Property Manager, Stennis Space Center, (228) 688-1929. Refer to SSC-00180.

Software Supports Distributed Operations via the Internet

Multi-mission Encrypted Communication System (MECS) is a computer program that enables authorized, geographically dispersed users to gain secure access to a common set of data files via the Internet. MECS is compatible with legacy application programs and a variety of operating systems. The MECS architecture is centered around maintaining consistent replicas of data files cached on remote computers. MECS monitors these files and, whenever one is changed, the changed file is committed to a master database as soon as network connectivity makes it possible to do so. MECS provides subscriptions for remote users to automatically receive new data as they are generated. Remote users can be producers as well as consumers of data. Whereas a prior program that provides some of the same services treats disconnection of a user from the network of users as an error from which re-

covery must be effected, MECS treats disconnection as a nominal state of the network: This leads to a different design that is more efficient for serving many users, each of whom typically connects and disconnects frequently and wants only a small fraction of the data at any given time.

This program was written by Jeffrey Norris, Paul Backes, and Robert Steinke of Caltech for NASA's Jet Propulsion Laboratory. Further information is contained in a TSP (see page 1).

In accordance with Public Law 96-517, the contractor has elected to retain title to this invention. Inquiries concerning rights for its commercial use should be addressed to

Intellectual Assets Office

JPL

Mail Stop 202-233

4800 Oak Grove Drive

Pasadena, CA 91109

(818) 354-2240

E-mail: ipgroup@jpl.nasa.gov

Refer to NPO-30448, volume and number of this NASA Tech Briefs issue, and the page number.

Software Estimates Costs of Testing Rocket Engines

Simulation-Based Cost Model (SiCM), a discrete event simulation developed in Extend™, simulates pertinent aspects of the testing of rocket propulsion test articles for the purpose of estimating the costs of such testing during time intervals specified by its users. A user enters input data for control of simulations; information on the nature of, and activity in, a given testing project; and information on resources. Simulation objects are created on the basis of this input. Costs of the engineering-design, construction, and testing phases of a given project are estimated from numbers and labor rates of engineers and technicians employed in each phase, the duration of each phase; costs of materials used in each phase; and, for the testing phase, the rate of maintenance of the testing facility. The three main outputs of SiCM are (1) a curve, updated at each iteration of the simulation, that shows overall expenditures vs. time during the interval specified by the user; (2) a histogram of the total costs from all iterations of the simulation; and (3) table displaying means and variances of cumulative costs

for each phase from all iterations. Other outputs include spending curves for each phase.

This program was written by C. L. Smith of Lockheed Martin Corp. for Stennis Space Center.

Inquiries concerning rights for the commercial use of this invention should be addressed to the Intellectual Property Manager, Stennis Space Center, (228) 688-1929. Refer to SSC-00168.

yourSky: Custom Sky-Image Mosaics via the Internet

yourSky (<http://yourSky.jpl.nasa.gov>) is a computer program that supplies custom astronomical image mosaics of sky regions specified by requesters using client computers connected to the Internet. [yourSky is an upgraded version of the software reported in "Software for Generating Mosaics of Astronomical Images" (NPO-21121), *NASA Tech Briefs*, Vol. 25, No. 4 (April 2001), page 16a.] A requester no longer has to engage in the tedious process of determining what subset of images is needed, nor even to know how the images are indexed in image archives. Instead, in response to a requester's specification of the size and location of the sky area, (and optionally of the desired set and type of data, resolution, coordinate system, projection, and image format), yourSky automatically retrieves the component image

data from archives totaling tens of terabytes stored on computer tape and disk drives at multiple sites and assembles the component images into a mosaic image by use of a high-performance parallel code. yourSky runs on the server computer where the mosaics are assembled. Because yourSky includes a Web-interface component, no special client software is needed: ordinary Web-browser software is sufficient.

This program was written by Joseph Jacob of Caltech for NASA's Jet Propulsion Laboratory. Further information is contained in a TSP (see page 1).

This software is available for commercial licensing. Please contact Don Hart of the California Institute of Technology at (818) 393-3425. Refer to NPO-30556.

Software for Managing Inventory of Flight Hardware

The Flight Hardware Support Request System (FHSRS) is a computer program that relieves engineers at Marshall Space Flight Center (MSFC) of most of the non-engineering administrative burden of managing an inventory of flight hardware. The FHSRS can also be adapted to perform similar functions for other organizations. The FHSRS affords a combination of capabilities, including those formerly provided by three separate pro-

grams in purchasing, inventorying, and inspecting hardware. The FHSRS provides a Web-based interface with a server computer that supports a relational database of inventory; electronic routing of requests and approvals; and electronic documentation from initial request through implementation of quality criteria, acquisition, receipt, inspection, storage, and final issue of flight materials and components. The database lists both hardware acquired for current projects and residual hardware from previous projects. The increased visibility of residual flight components provided by the FHSRS has dramatically improved the re-utilization of materials in lieu of new procurements, resulting in a cost savings of over \$1.7 million. The FHSRS includes sub-programs for manipulating the data in the database, informing of the status of a request or an item of hardware, and searching the database on any physical or other technical characteristic of a component or material. The software structure forces normalization of the data to facilitate inquiries and searches for which users have entered mixed or inconsistent values.

This program was designed and written by John Salisbury, Scott Savage, and Shirman Thomas of Cortez III for Marshall Space Flight Center. Further information is contained in a TSP (see page 1). MFS-31661



Lower-Conductivity Thermal-Barrier Coatings

Additional stabilizers are incorporated into yttria-stabilized zirconia.

John H. Glenn Research Center, Cleveland, Ohio

Thermal-barrier coatings (TBCs) that have both initial and post-exposure thermal conductivities lower than those of yttria-stabilized zirconia TBCs have been developed. TBCs are thin ceramic layers, generally applied by plasma spraying or physical vapor deposition, that are used to insulate air-cooled metallic components from hot gases in gas turbine and other heat engines. Heretofore, yttria-stabilized zirconia (nominally comprising 95.4 atomic percent ZrO_2 + 4.6 atomic percent Y_2O_3) has been the TBC material of choice. The lower-thermal-conductivity TBCs are modified versions of yttria-stabilized zirconia, the modifications consisting primarily in the addition of other oxides that impart microstructural and defect properties that favor lower thermal conductivity.

TBCs are characterized by porosity, typically between 5 and 20 percent. Porosity reduces the thermal conductivity of a TBC below the intrinsic conductivity of a fully dense (that is, non-porous) layer of the TBC material. The thermal conductivity of a TBC increases as its porosity is reduced by the sintering that occurs during use at high temperature. For future engines that will operate at higher gas temperatures, TBCs with greater degrees of both initial insulating

capability and retention of insulating capability will be needed.

The present lower-thermal-conductivity TBCs are made of Zr_2O_2 and Y_2O_3 doped with additional oxides that are chosen to perform three functions:

- Create thermodynamically stable, highly defective lattice structures with tailored ranges of defect-cluster sizes to exploit the effectiveness of such structures as means of attenuating and scattering phonons, thus reducing thermal conductivity;
- Produce of highly distorted lattice structures with essentially immobile defect clusters and/or nanoscale ordered phases, which effectively reduces concentrations of mobile defects and movements of atoms, thus increasing sintering-creep resistance; and
- Exploit the formation of complex nanoscale clusters of defects to increase the measures of such desired mechanical properties such as fracture toughness.

The additional oxides in a TBC according to this concept are typically selected as a pair — one from each of two groups of oxides denoted for this purpose as groups A and B. Group A includes scandia (Sc_2O_3) and ytterbia (Yb_2O_3). These oxides are highly stable, and the radii of their trivalent cations are smaller than

those of the primary dopant yttria. Group B includes neodymia (Nd_2O_3), samaria (Sm_2O_3), and gadolinia (Gd_2O_3) which are also highly stable, and their trivalent cations are larger than those of yttria.

Like yttria, the A and B oxides are regarded as stabilizers. Preferably, the total stabilizer content (yttria + A oxide + B oxide) should lie between 4 and 50 atomic percent. The concentration of yttria should exceed that of each of other stabilizers, and the concentrations of the A and B oxides should be approximately equal. Formulations other than the foregoing preferred one are also possible: Variations include the use of alternative group-A oxides (e.g., MgO_2 , NiO , Cr_2O_3), the use of two or more group-A and/or group-B oxides, substitution of hafnia for zirconia, and substitution of other primary stabilizers (e.g., dysprosia or erbia) for yttria.

This work was done by Robert A. Miller of Glenn Research Center and Dongming Zhu of Ohio Aerospace Institute. Further information is contained in a TSP (see page 1).

Inquiries concerning rights for the commercial use of this invention should be addressed to NASA Glenn Research Center, Commercial Technology Office, Attn: Steve Fedor, Mail Stop 4-8, 21000 Brookpark Road, Cleveland, Ohio 44135. Refer to LEW-17039.

Process for Smoothing an Si Substrate After Etching of SiO_2

Reactive-ion etching can be tailored to minimize undesired side effects.

NASA's Jet Propulsion Laboratory, Pasadena, California

A reactive-ion etching (RIE) process for smoothing a silicon substrate has been devised. The process is especially useful for smoothing those silicon areas that have been exposed by etching a pattern of holes in a layer of silicon dioxide that covers the substrate. Applications in which one could utilize smooth silicon surfaces like those produced by this process include fabrication of optical waveguides, epitaxial deposition of silicon on selected areas of silicon substrates, and prepara-

tion of silicon substrates for deposition of adherent metal layers.

During etching away of a layer of SiO_2 that covers an Si substrate, a polymer becomes deposited on the substrate, and the substrate surface becomes rough (roughness height ≈ 50 nm) as a result of over-etching or of deposition of the polymer. While it is possible to smooth a silicon substrate by wet chemical etching, the undesired consequences of wet chemical etching can include compro-

promising the integrity of the SiO_2 sidewalls and undercutting of the adjacent areas of the silicon dioxide that are meant to be left intact.

The present RIE process results in anisotropic etching that removes the polymer and reduces height of roughness of the silicon substrate to <10 nm while leaving the SiO_2 sidewalls intact and vertical. Control over substrate versus sidewall etching (in particular, preferential etching of the substrate) is

achieved through selection of process parameters, including gas flow, power, and pressure. Such control is not uniformly and repeatably achievable in wet chemical etching. The recipe for the present RIE process is the following:

Etch 1 — A mixture of CF_4 and O_2 gases flowing at rates of 25 to 75 and 75 to 125 standard cubic centimeters per minute ($\text{stdcm}^3/\text{min}$), respectively; power between 44 and 55 W; and pressure between 45 and 55 mtorr (between

6.0 and 7.3 Pa). The etch rate lies between ≈ 3 and ≈ 6 nm/minute.

Etch 2 — O_2 gas flowing at 75 to 125 $\text{stdcm}^3/\text{min}$, power between 44 and 55 W, and pressure between 50 and 100 mtorr (between 6.7 and 13.3 Pa).

This work was done by Tasha Turner and Chi Wu of Caltech for NASA's Jet Propulsion Laboratory. Further information is contained in a TSP (see page 1).

In accordance with Public Law 96-517, the contractor has elected to retain title to this

invention. Inquiries concerning rights for its commercial use should be addressed to

Intellectual Property group

JPL

Mail Stop 202-233

4800 Oak Grove Drive

Pasadena, CA 91109

(818) 354-2240

Refer to NPO-20777, volume and number of this NASA Tech Briefs issue, and the page number.

Flexible Composite-Material Pressure Vessel

Lyndon B. Johnson Space Center, Houston, Texas

A proposed lightweight pressure vessel would be made of a composite of high-tenacity continuous fibers and a flexible matrix material. The flexibility of this pressure vessel would render it (1) compactly stowable for transport and (2) more able to withstand impacts, relative to lightweight pressure vessels made of rigid composite materials. The vessel would be designed as a structural shell wherein the fibers would be predominantly bias-oriented, the orienta-

tions being optimized to make the fibers bear the tensile loads in the structure. Such efficient use of tension-bearing fibers would minimize or eliminate the need for stitching and fill (weft) fibers for strength. The vessel could be fabricated by techniques adapted from filament winding of prior composite-material vessels, perhaps in conjunction with the use of dry film adhesives. In addition to the high-bias main-body substructure described above, the vessel would in-

clude a low-bias end substructure to complete coverage and react peak loads. Axial elements would be overlaid to contain damage and to control fiber orientation around side openings. Fiber ring structures would be used as interfaces for connection to ancillary hardware.

This work was done by Glen Brown, Roy Haggard, and Paul A. Harris of Vertigo, Inc., for Johnson Space Center. Further information is contained in a TSP (see page 1).
MSC-23020

Treatment To Destroy Chlorohydrocarbon Liquids in the Ground

Emulsified iron is injected into the ground and left there.

John F. Kennedy Space Center, Florida

A relatively simple chemical treatment that involves the use of emulsified iron has been found to be effective in remediating groundwater contaminated with trichloroethylene and other dense chlorohydrocarbon liquids. These liquids are members of the class of dense, non-aqueous phase liquids (DNAPLs), which are commonly recognized to be particularly troublesome as environmental contaminants. The treatment converts these liquids into less-harmful products.

As a means of remediation of contaminated groundwater, this treatment takes less time and costs less than do traditional pump-and-treat processes. At some sites, long-term leakage and/or dissolution of chlorohydrocarbon liquids from pools and/or sorbed concentrations in rock and soil gives rise to a need to continue pump-and-treat processes for times as long as decades in order to maintain protection of human health and the environment. In contrast, the effects of the emulsified-iron

treatment are more lasting, decreasing the need for long-term treatment and monitoring of contaminated areas.

The material used in this treatment consists of iron particles with sizes of the order of nanometers to micrometers contained within the micelles of a surfactant-stabilized, biodegradable, oil-in-water emulsion. The emulsion is simple to prepare and consists of relatively inexpensive and environmentally acceptable ingredients: One typical formulation consists of 1.3 weight percent of a food-grade surfactant, 17.5 weight percent of iron particles, 23.2 weight percent of vegetable oil, and 58.0 weight percent of water.

The emulsion is injected into the ground via a push well. Free-phase chlorohydrocarbon molecules diffuse through the oil membranes of the emulsion particles to the surfaces of the iron particles, where dehalogenation takes place. The dehalogenation reactions generate hydrocarbon byproducts (primarily

ethylene in the case of trichloroethylene), which diffuse out of the emulsion micelles and are benign in nature.

Experiments have demonstrated several aspects of the effectiveness of this treatment by use of emulsified iron:

- This treatment is more effective in degrading free-phase trichloroethylene than is a similar treatment that uses only pure iron particles.
- Emulsions containing iron can be injected into soil matrices, where they become immobilized and remain immobile, even in the presence of flowing water.
- Iron emulsions can exert an effect equivalent to pulling globules of trichloroethylene into their micelles.
- No chlorinated byproducts from the degradation of trichloroethylene pass out of the micelles. The only degradation products that have been observed to leave the iron emulsions are ethylene as mentioned previously,

plus trace amounts of other innocuous hydrocarbons.

Laboratory studies have shown that the amount of emulsion needed to degrade a given amount of trichloroethylene is approximately eight times the mass of the trichloroethylene. Because there are no continuing operating costs after the emulsion has been injected through push

wells, the iron-emulsion treatment offers a substantial economic advantage over the long-term pump-and-treat method.

*This work was done by Jacqueline Quinn of **Kennedy Space Center** and Christian A. Clausen III, Cherie L. Geiger, Debra Reinhart, and Kathleen Brooks of the University of Central Florida. Further information is contained in a TSP (see page 1).*

This invention is owned by NASA, and a patent application has been filed. Inquiries concerning nonexclusive or exclusive license for its commercial development should be addressed to the Technology Commercialization Office, Kennedy Space Center, (321) 867-8130. Refer to KSC-12246.



Noncircular Cross Sections Could Enhance Mixing in Sprays

Preliminary results suggest that elliptical cross sections may be best.

NASA's Jet Propulsion Laboratory, Pasadena, California

A computational study has shown that by injecting drops in jets of gas having square, elliptical, triangular, or other noncircular injection cross sections, it should be possible to increase (relative to comparable situations having circular cross section) the entrainment and dispersion of liquid drops. This finding has practical significance for a variety of applications in which it is desirable to increase dispersion of drops. For example,

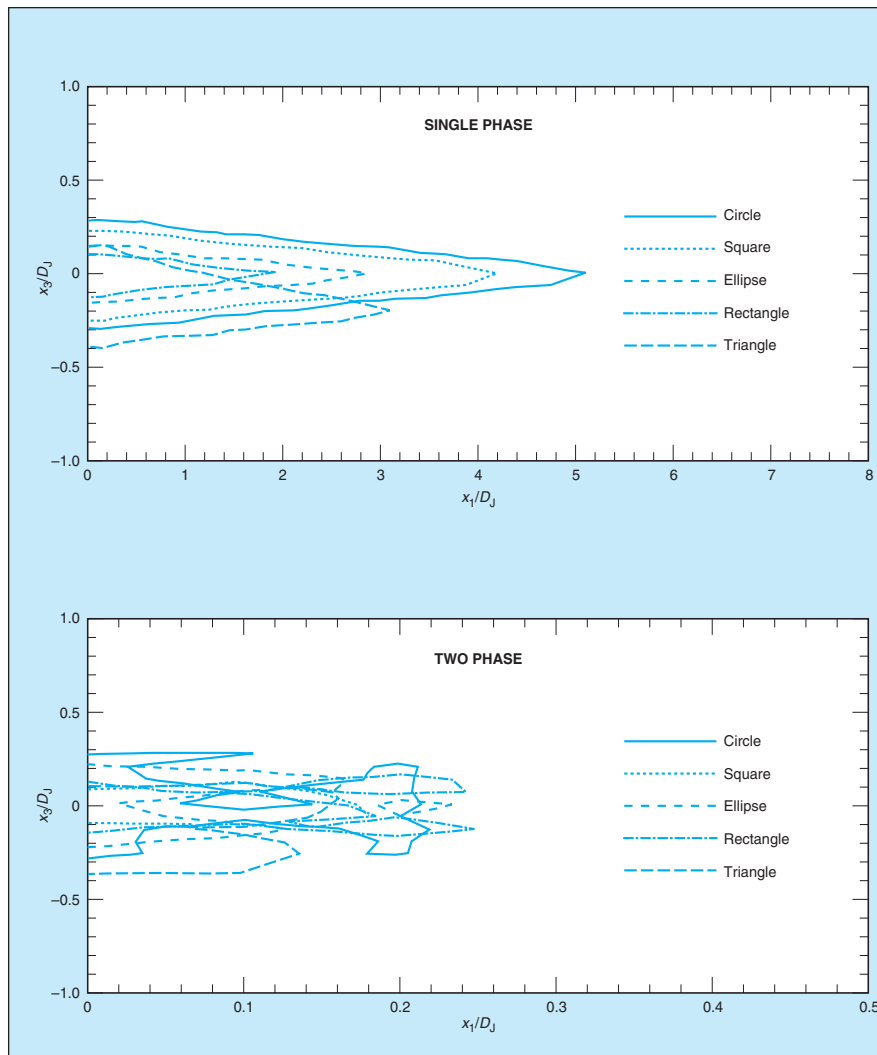
in chemical-process sprays, increased dispersion leads to increases in chemical-reaction rates; in diesel engines, increasing the dispersion of drops of sprayed fuel reduces the production of soot; and in household and paint sprays, increasing the dispersion of drops makes it possible to cover larger surfaces.

It has been known for some years that single-phase fluid jets that enter flow

fields through noncircular inlets entrain more fluid than do comparable jets entering through circular inlets. The computational study reported here was directed in part toward determining whether and how this superior mixing characteristic of noncircular single-phase jets translates to a similar benefit in cases of two-phase jets (that is, sprays).

The study involved direct numerical simulations of single- and two-phase free jets with circular, elliptical, rectangular, square, and triangular inlet cross sections. The two-phase jets consisted of gas laden with liquid drops randomly injected at the inlets. To address the more interesting case of evaporating drops, the carrier gas in the jets was specified to be initially unvitiated by the vapor of the liquid chemical species and the initial temperature of the drops was chosen to be smaller than that of the gas. The mathematical model used in the study was constructed from the conservation equations for the two-phase flow and included complete couplings of mass, momentum, and energy based on thermodynamically self-consistent specification of the enthalpy, internal energy, and latent heat of vaporization of the vapor.

The results of the numerical simulations yielded information on (1) the different spreading behaviors occurring for different inlet cross sections and (2) the differences between flow fields in the presence and absence of liquid drops. The most important consequence of interaction of drops with the flows was found to be the production of enhanced streamwise vorticity that alters entrainment and the mixing of species according to the inlet geometry. At the time station corresponding to steady-state entrainment, the potential cores of two-phase jets were found to be shorter than their single-phase counterparts by an order of magnitude (see figure). Whereas the two-phase circular jets were found to exhibit symmetric entrainment patterns at a location well past the streamwise locations of the potential cores, the noncircular jets were found, at the same location, to depart strongly from symmetry. The phenomenon of



The **Potential Core** of a jet is defined as the region beyond which the velocity is no longer equal to that at the inlet. These plots are outlines of computationally simulated potential cores of single- and two-phase jets issuing from inlets with the noted cross sections. D_j denotes the equivalent jet diameter, which, for a noncircular inlet, is defined as the diameter of a circular inlet of equal cross-sectional area. The symbols x_1 and x_3 denote Cartesian coordinates parallel and perpendicular, respectively, to the initial jet axis.

upstream-vs.-downstream exchange of major and minor axes of elliptical cross sections (“axis switching” for short) of single-phase jets was not observed in the two-phase jets.

Considerations of the distributions of the number density of drops, liquid mass, and evaporated species distribu-

tions lead to recommending elliptical cross sections as optimal ones in that they result in optimal combinations of dispersion and mixing. All of the computations were performed for pre-transitional jets (that is, jets on the laminar side of the transition between laminar and turbulent flow). Further investiga-

tions would be necessary to elucidate the effects of turbulence.

*This work was done by Josette Bellan and Hesham Abdel-Hameed of Caltech for NASA’s Jet Propulsion Laboratory. Further information is contained in a TSP (see page 1).
NPO-30400*



Small, Untethered, Mobile Robots for Inspecting Gas Pipes

These robots would be powered by gas flows.

NASA's Jet Propulsion Laboratory, Pasadena, California

Small, untethered mobile robots denoted gas-pipe explorers (GPEXs) have been proposed for inspecting the interiors of pipes used in the local distribution natural gas. The United States has network of gas-distribution pipes with a total length of approximately 10^9 m. These pipes are often made of iron and steel and some are more than 100 years old. As this network ages, there is a need to locate weaknesses that necessitate repair and/or preventive maintenance. The most common weaknesses are leaks and reductions in thickness, which are caused mostly by chemical reactions between the iron in the pipes and various substances in soil and groundwater.

At present, mobile robots called pigs are used to inspect and clean the interiors of gas-transmission pipelines. Some carry magnetic-flux-leakage (MFL) sensors for measuring average wall thicknesses, some capture images, and some measure sizes and physical conditions. The operating ranges of pigs are limited to fairly straight sections of wide transmission-type (as distinguished from distribution-type) pipes: pigs are too large to negotiate such obstacles as bends with radii comparable to or smaller than pipe diameters, intrusions of other pipes at branch connections, and reductions in diameter at valves and meters. The GPEXs would be smaller and would be able to negotiate sharp bends and other obstacles that typically occur in gas-distribution pipes.

Unlike a pig, a GPEX would be able to operate or even fail inside a pipe without stopping the gas flow. It would be capable

of operating for long times and traveling long distances without human intervention, so that expensive and disruptive urban excavation could be kept to a minimum; to make this possible, the GPEX would generate its own power from the flow of gas. It would communicate information, including low-rate data like those from an MFL sensor and high-rate image data that show corrosion, leaks, and buckles. Two-way radio communication, for both retrieval of inspection data and control of the GPEX, would take place at gigahertz carrier frequencies, with pipes serving as waveguides. The GPEX must transform its shape as needed to cope with changes in pipe dimensions, dents, pipe bends, and pipe intrusions.

A prototype GPEX that would be capable of operating inside either a 4-in. (10-cm) or a 6-in. (15-cm) pipe has been developed. At present, it is viewed as infeasible to package all the needed functions of the GPEX inside a single body that could negotiate right-angle turns in a 10-cm pipe. Therefore, the prototype GPEX is composed of a train of multiple units, much like a railroad train. Because the source of power would be the flow of natural gas in the pipe to be inspected, the first unit in the train would be a combination of a power generator and locomotive. The flow of gas [typically methane at a flow speed of 10 m/s, a pressure of 60 psi (≈ 0.4 MPa), and a temperature of 15 °C] could supply sufficient power to enable the robot to perform all its tasks, without a major loss of gas pressure.

The initial development effort is expected to focus on the power-genera-

tor/locomotive unit. The power generator would be a permanent-magnet motor back-driven by a miniature turbine driven by the flow of gas. In normal operation, power of at least 2 W would be required, and the pressure drop would have to be limited to no more than 0.3 psi (2 kPa). A further requirement is that in the event of worst-case failure of the generator or any other part of the GPEX, the pressure drop not exceed 0.6 psi (4 kPa).

The power-generator/locomotive unit is a pair of bodies connected by an extension actuator. Multiple bladders can be alternately inflated and deflated to exert forces on the pipe wall, and the extension actuator can increase or decrease the separation between the bodies to move the unit in "inchworm" fashion.

This work was done by Brian Wilcox of Caltech for NASA's Jet Propulsion Laboratory. Further information is contained in a TSP (see page 1).

In accordance with Public Law 96-517, the contractor has elected to retain title to this invention. Inquiries concerning rights for its commercial use should be addressed to

Intellectual Assets Office

JPL

Mail Stop 202-233

4800 Oak Grove Drive

Pasadena, CA 91109

(818) 354-2240

E-mail: ipgroup@jpl.nasa.gov

Refer to NPO-20991, volume and number of this NASA Tech Briefs issue, and the page number.

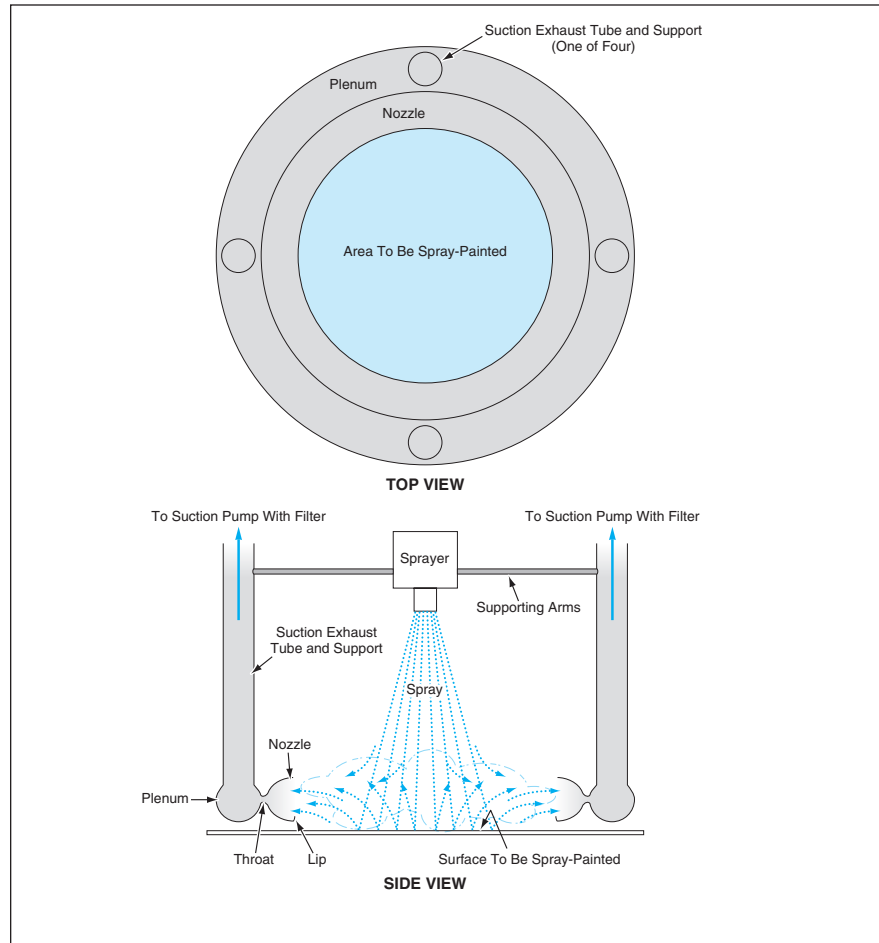
Paint-Overspray Catcher

Turning airflow and entrained droplets would be drawn away.

Langley Research Center, Hampton, Virginia

An apparatus to catch paint overspray has been proposed. Overspray is an unavoidable parasitic component of spray that occurs because the flow of air or other

gas in the spray must turn at the sprayed surface. Very small droplets are carried away in this turning flow, and some land on adjacent surfaces not meant to be painted.



The **Paint-Overspray Catcher** would suck the turning flow of gas and entrained paint droplets, preventing the droplets from landing on non-target surfaces. The planform of the catcher plenum and nozzle need not be round as shown here: It could have any other convenient shape, depending on the boundary of the area to be painted.

The basic principle of the paint-spray catcher is to divert the overspray into a suction system at the boundary of the area to be painted. The paint-spray catcher (see figure) would include a toroidal plenum connected through narrow throat to a nozzle that would face toward the center of the torus, which would be positioned over the center of the area to be spray-painted. The plenum would be supported by four tubes that would also serve as suction exhaust ducts. The downstream ends of the tubes (not shown in the figure) would be connected to a filter on a suction pump. The pump would be rated to provide a suction mass flow somewhat greater than that of the directed spray gas stream, so that the nozzle would take in a small excess of surrounding gas and catch nearly all of the overspray. A small raised lip at the bottom edge of the nozzle would catch paint that landed inside the nozzle. Even if the paint is directly piston pumped, the droplets entrain an air flow by time they approach the wall, so there is always a gas stream to carry the excess droplets to the side. For long-duration spraying operations, it could be desirable to include a suction-drain apparatus to prevent overflowing and dripping of paint from inside the lip. A version without an external contraction and with the throat angled downward would be a more compact version of catcher, although it might be slightly less efficient.

This work was done by Leonard M. Weinstein of Langley Research Center. For more information, contact the Langley Commercial Technology Office at (757) 864-6005. LAR-15613

Preparation of Regular Specimens for Atom Probes

Single- or multiple-tip specimens can readily be prepared.

NASA's Jet Propulsion Laboratory, Pasadena, California

A method of preparation of specimens of non-electropolishable materials for analysis by atom probes is being developed as a superior alternative to a prior method. In comparison with the

prior method, the present method involves less processing time. Also, whereas the prior method yields irregularly shaped and sized specimens, the present developmental method offers

the potential to prepare specimens of regular shape and size.

The prior method is called the method of sharp shards because it involves crushing the material of interest

and selecting microscopic sharp shards of the material for use as specimens. Each selected shard is oriented with its sharp tip facing away from the tip of a stainless-steel pin and is glued to the tip of the pin by use of silver epoxy. Then the shard is milled by use of a focused ion beam (FIB) to make the shard very thin (relative to its length) and to make its tip sharp enough for atom-probe analysis. The method of sharp shards is extremely time-consuming because the selection of shards must be performed with the help of a microscope, the shards must be positioned on the pins by use of micromanipulators, and the irregularity of size and shape necessitates many hours of FIB milling to sharpen each shard.

In the present method, a flat slab of the material of interest (e.g., a polished sample of rock or a coated semiconductor wafer) is mounted in the sample holder of a dicing saw of the type conventionally used to cut individual inte-

grated circuits out of the wafers on which they are fabricated in batches. A saw blade appropriate to the material of interest is selected. The depth of cut and the distance between successive parallel cuts is made such that what is left after the cuts is a series of thin, parallel ridges on a solid base. Then the workpiece is rotated 90° and the pattern of cuts is repeated, leaving behind a square array of square posts on the solid base.

The posts can be made regular, long, and thin, as required for samples for atom-probe analysis. Because of their small volume and regularity, the amount of FIB-milling time can be much less than that of the method of sharp shards. Individual posts can be broken off for mounting in a manner similar to that of the method of sharp shards. Alternatively, the posts can be left intact on the base and the base can be cut to a small square (e.g., 3 by 3 mm) suitable for mounting in an atom probe of a type ca-

pable of accepting multiple-tip specimens. The advantage of multiple-tip specimens is the possibility of analyzing many tips without the time-consuming interchange of specimens.

This work was done by Kim Kuhlman and James Wishard of Caltech for NASA's Jet Propulsion Laboratory. Further information is contained in a TSP (see page 1).

In accordance with Public Law 96-517, the contractor has elected to retain title to this invention. Inquiries concerning rights for its commercial use should be addressed to

Intellectual Assets Office

JPL

Mail Stop 202-233

4800 Oak Grove Drive

Pasadena, CA 91109-8099

(818) 354-2240

E-mail: ipgroupp@jpl.nasa.gov

Refer to NPO-30667, volume and number of this NASA Tech Briefs issue, and the page number.

Inverse Tomo-Lithography for Making Microscopic 3D Parts

Inverse tomography would be used to generate complex three-dimensional patterns.

NASA's Jet Propulsion Laboratory, Pasadena, California

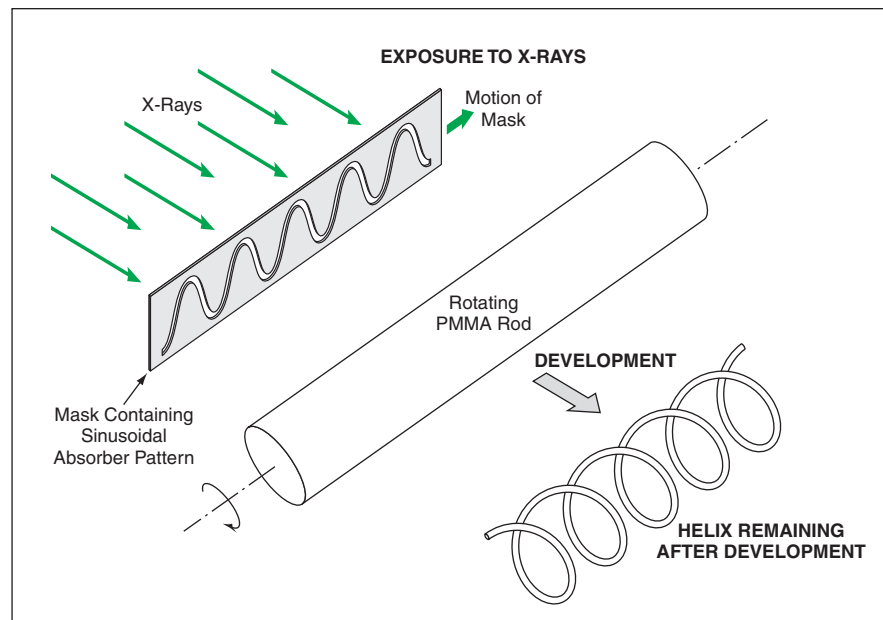
According to a proposal, basic x-ray lithography would be extended to incorporate a technique, called "inverse tomography," that would enable the fabrication of microscopic three-dimensional (3D) objects. The proposed inverse tomo-lithographic process would make it possible to produce complex shaped, submillimeter-sized parts that would be difficult or impossible to make in any other way. Examples of such shapes or parts include tapered helices, paraboloids with axes of different lengths, and even Archimedean screws that could serve as rotors in microturbines.

The proposed inverse tomo-lithographic process would be based partly on a prior microfabrication process known by the German acronym "LIGA" ("lithographie, galvanofornung, abformung," which means "lithography, electroforming, molding"). In LIGA, one generates a precise, high-aspect ratio pattern by exposing a thick, x-ray-sensitive resist material to an x-ray beam through a mask that contains the pattern. One can electrodeposit metal into the developed resist pattern to form a precise metal part, then dissolve the resist to free the metal. Aspect ratios of

100:1 and patterns into resist thicknesses of several millimeters are possible.

Typically, high-molecular-weight poly (methyl methacrylate) (PMMA) is used as the resist material. PMMA is an excellent

resist material in most respects, its major shortcoming being insensitivity. Conventional x-ray sources are not practical for LIGA work, and it is necessary to use a synchrotron as the source. Because syn-



A Rotating PMMA Rod would be exposed to collimated x-rays through a mask bearing a sinusoidal absorber pattern while the mask moved along the rod in synchronism with the rotation. Upon development of the PMMA (used here as an x-ray photoresist material), a helix would remain.

chrotron radiation is highly collimated and its wavelength of synchrotron radiation is typically $<5 \text{ \AA}$, there is very little diffraction and the pattern of a high-contrast mask is projected deep into a resist with nearly perfect vertical sidewalls. Of course, the only three-dimensional shape that can be formed in this way is the locus of points generated by moving the mask pattern along the direction of incidence of the radiation.

In a recently developed variant of LIGA, a rotating PMMA rod is exposed to x-rays through a stationary mask; this technique can be used to make axisymmetric structures; e.g., objects shaped like wine glasses or baseball bats. The proposed technique would also involve stenciling an x-ray image into a rotating PMMA rod, but would differ from prior techniques in

that the mask would be moved in synchronism with the rod to generate a three-dimensional pattern. The synchronized motions of the mask and rod would be generated by translation and rotation stages actuated by stepping motors under control by a computer.

Describing the x-ray exposure technique in different words, a changing two-dimensional pattern would be projected into a three-dimensional one. In tomography, one decodes a three-dimensional pattern from the changing two-dimensional pattern obtained by illuminating it from a changing direction. In the proposed technique, one would essentially reverse this decoding process; that is, one would encode or construct a three-dimensional pattern by illuminating the region of interest in a changing

two-dimensional pattern: That is why the proposed x-ray exposure technique is called "inverse tomography."

The figure depicts an example of the use of this technique to generate a simple helix. The two-dimensional projection (shadow) of a helix is a sinusoid. To form the helical pattern in a PMMA rod, one would project x-rays perpendicularly toward the rod through a mask with a sinusoidal pattern while rotating the rod and translating the mask along the rod at a speed of one wavelength of the sinusoid per rotation period.

This work was done by Victor White and Dean Wiberg of Caltech for NASA's Jet Propulsion Laboratory. Further information is contained in a TSP (see page 1). NPO-20593



Predicting and Preventing Incipient Flameout in Combustors

Increases in acoustic signals could trigger rapid adjustments to prevent flameouts.

Langley Research Center, Hampton, Virginia

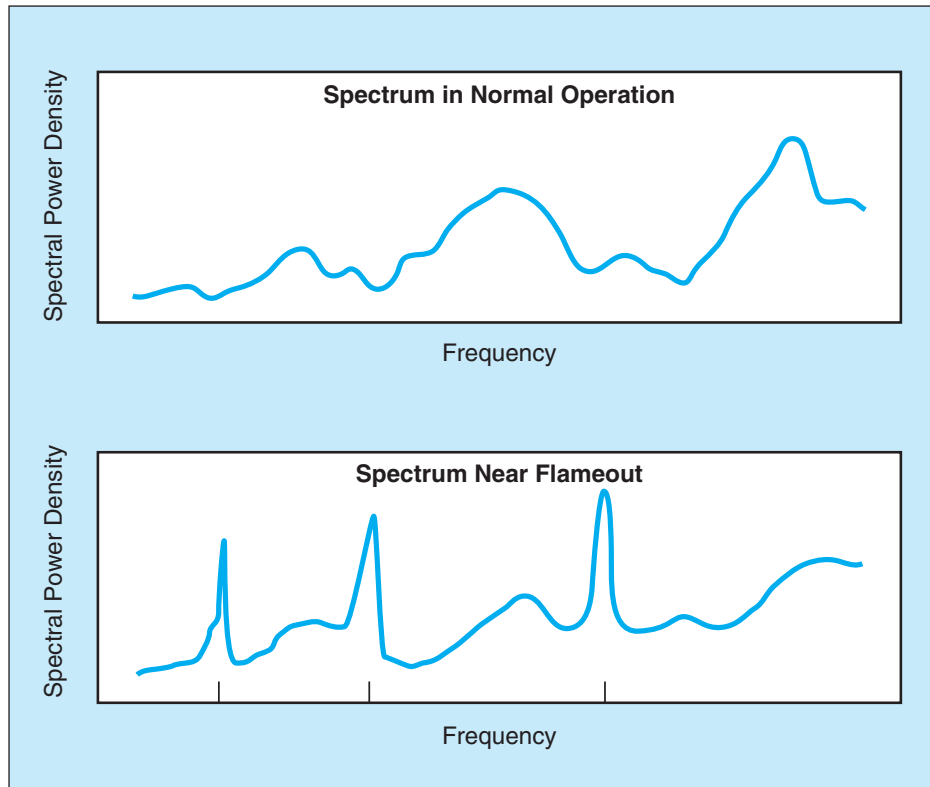
A method of predicting and preventing incipient flameout in a combustor has been proposed. The method should be applicable to a variety of liquid- and gas-fueled combustors in furnaces and turbine engines. Until now, there have been methods of detecting flameouts after they have occurred, but there has been no way of predicting incipient flameouts and, hence, no way of acting in time to prevent them. Prevention of flameout could not only prevent damage to equipment but, in the case of aircraft turbine engines, could also save lives.

For any combustor, excessive departure from optimum operating conditions can lead to instability that quickly ends in flameout. Of particular interest is that for a given temperature and pressure of incoming air, flameout can occur if the fuel/air ratio is too high or too low. In many cases, combustors are operated nearer their lean-mixture (low fuel/air ratio) stability boundaries.

Studies have shown that as a combustor approaches instability, pressure fluctuations increase sharply. One measure of such fluctuations that has been found to be especially useful is the ratio between the magnitude of pressure fluctuations (essentially, the acoustic pressure) and the time-averaged pressure. Alternatively, one could detect instability-related pressure fluctuations by detecting the sudden appearance of one or more acoustic spectral peak(s) at frequencies known to be associated with instabilities in the particular combustor (see figure).

The proposed method is based largely on the foregoing observations. It calls for continuous monitoring and analysis of the acoustic pressure and several other key physical parameters that are indicative of the state of the combustion process. The instrumentation needed to implement the method in a typical installation would include the following:

- Meters to measure the flows of fuel and air into the combustor;
- Gauges to measure the pressures of the entering fuel and air;



Strong Peaks associated with instability appear in the acoustic spectrum of a combustor as it approaches flameout. The frequencies and amplitudes of the peaks depend on the combustor geometry and on temperature.

- Thermocouples to measure the temperatures of the entering fuel and air;
- One or more thermocouple(s) to measure the temperature(s) at a key location or locations in the combustor;
- A microphone or other acoustic-pressure transducer;
- Analog-to-digital converters for sampling the outputs of the aforementioned sensors;
- A computer running special software for analyzing the digitized sensor outputs and responding as needed;
- Digital-to-analog converters to generate actuator-control signals for automated rapid responses; and
- Output connections to displays that would be read by human operators.

Through continuous monitoring of the temperatures, pressures, and flow rates, the instrumentation system would provide information that would

enable a pilot, power-plant operator, or other responsible person to set the flow rates of fuel and air for safe operation. Upon detecting a sudden large increase in acoustic pressure, the system would act, much faster than the human operator could, to make a temporary adjustment in the fuel/air ratio to prevent flameout. For example, if the combustor was operating near the lean stability boundary, the system could respond by actuating a solenoid valve or fuel injector to increase the flow of fuel. At the same time, the system would generate a display advising the human operator of this action and suggesting an adjustment to restore steady safe operation.

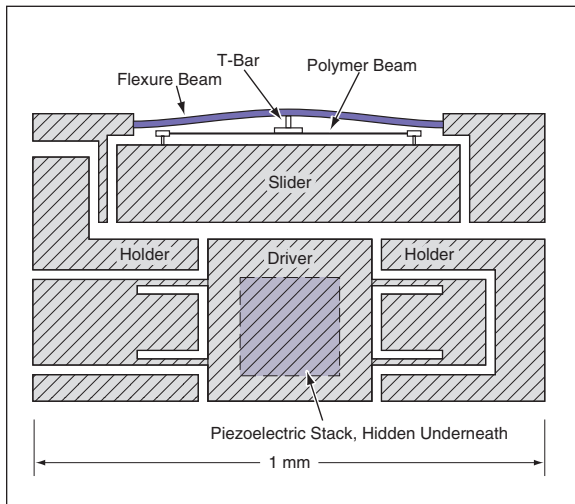
This work was done by Richard Lee Puster of Langley Research Center. Further information is contained in a TSP (see page 1). LAR-15487

MEMS-Based Piezoelectric/Electrostatic Inchworm Actuator

Nanometer steps could be concatenated into overall travel of hundreds of microns.

NASA's Jet Propulsion Laboratory, Pasadena, California

A proposed inchworm actuator, to be designed and fabricated according to the principles of microelectromechanical systems (MEMS), would effect linear motion characterized by steps as small as nanometers and an overall range of travel of hundreds of microns. Potential applications for actuators like this one include precise positioning of optical components and active suppression of noise and vibration in scientific instruments, conveyance of wafers in the semiconductor industry, precise positioning for machine tools, and positioning and actuation of microsurgical instruments.



This Piezoelectric/Electrostatic Actuator would produce motion of the slider into or out of the page in small increments.

The inchworm motion would be generated by a combination of piezoelectric driving and electrostatic clamping. The actuator (see figure), would include a pair of holders (used for electrostatic clamping), a slider (the part that would engage in the desired linear motion), a driver, a piezoelectric stack under the driver, and a pair of polymer beams centrally clamped to the flexure beam via a T bar. The holders would be held stationary. One end of the piezoelectric stack would be held stationary; the other end would be connected to the bottom of the driver, which would be free to move up and down. All of these components except the piezoelectric stack and the polymer beams would be micromachined from a 500- μm -thick silicon wafer by deep reactive-ion etching. The inchworm motion would be perpendicular to the broad faces of the wafer (perpendicular to the plane of the figure).

The combination of the polymer beams and the centrally clamped flexure beam would spring-bias the slider into a position such that, in the absence of electrostatic clamping, the gap between the slider on the one hand and both the

driver and the holder on the other hand would be no more than a few microns. This arrangement would make it possible to electrostatically pull the slider into contact with either the holders or the driver at a clamping force of the order of 1 N by applying a reasonably small voltage (of the order of 100 V).

The actuation sequence would be the following:

1. The slider would be electrostatically clamped to the driver.
2. The piezoelectric stack would push the driver upward or downward (out of or into the page, respectively).
3. The slider would be electrostatically clamped to the holders.
4. The slider and the driver would be released from each other.
5. The driver would be moved downward or upward by the piezoelectric actuator while the slider remained clamped to the holders. This would complete the sequence for one increment of motion.
6. The cycle comprising steps 1 through 5 would be repeated as many times as needed to obtain the desired overall upward or downward travel. The repetition rate could be as high as about 1 kHz.

This work was done by Eui-Hyeok Yang of Caltech for NASA's Jet Propulsion Laboratory. Further information is contained in a TSP (see page 1).
NPO-30672

Metallized Capillaries as Probes for Raman Spectroscopy

These would offer several advantages over fiber-optic probes.

NASA's Jet Propulsion Laboratory, Pasadena, California

A class of miniature probes has been proposed to supplant the fiber-optic probes used heretofore in some Raman and fluorescence spectroscopic systems. A probe according to the proposal would include a capillary tube coated with metal on its inside to make it reflective. A microlens would be hermetically sealed onto one end of the tube. A spectroscopic probe head would contain a single such probe, which would both deliver laser light to a sample and collect Raman or fluorescent light emitted by the sample.

The capabilities of most prior Raman and fluorescence fiber-optic probes are limited because of spurious emission of Raman and fluorescent light by the cores of the optical fibers themselves. To prevent the spurious emissions from overwhelming the desired Raman and/or fluorescence signals, it is necessary to incorporate spectral filters. In a given application, such a filter undesirably limits the probe to a single laser wavelength. Filtration is usually performed by means of free-space optics in the probe head.

These optics are vulnerable to misalignment. Alternatively, thin-film filters can be deposited directly on optical fibers or in proximity to the fibers, but the performances of such filters are inferior to those of free-space optical filters.

A typical probe according to the proposal would have an outside diameter of <1 mm. Relative to a typical prior Raman probe, this probe would be much smaller and lighter and could be manufactured at lower cost. The interior of the probe could be evacuated or filled

with a gas (e.g., argon) that does not emit any Raman or fluorescent light in the spectral region of interest. Hence, there would be no need for filters, ancillary filter optics, and associated mounting hardware vulnerable to misalignment, and so the probe would be better able to withstand such adverse environmental conditions as higher pressures, temperatures, and mechanical shocks. The elimination of filters would make it possible to operate the probe at more than one wavelength. A probe according to the proposal could perform well in the deep ultraviolet spectral region, which is important for spectral detection of organisms. Unlike fiber-optic probes containing filters, these probes could be used to measure Raman wave-number shifts smaller than 50 cm^{-1} .

In the development of these probes, it should be possible to take advantage of the knowledge base already accumulated in the use of metallized capillary

tubes to deliver laser beams for surgery and cutting metal. Provided that the reflectivity of the interior metal coat of a capillary is sufficiently high, the numerical aperture of the capillary sufficiently low, and the diameter of the capillary sufficiently large, it should be possible to achieve efficient transmission of light along the capillary.

The small size, low cost, and multi-wavelength capability of these probes make them attractive for many Raman and fluorescence applications. Matrices of samples generated by combinatorial chemistry could be analyzed by an array of these probes interfaced to a single fiber-optic probe head or directly to a single Raman spectrograph. Access ports to chemical reactors could be kept small, reducing the potential hazards of a seal failure. Probes inserted into large chemical reactors could be much smaller in diameter due to the greatly relaxed stiffness requirements compared

to traditional Raman probes. Also, because of their smallness, they would be capable of withstanding high pressures and would be well suited for use in undersea exploration.

This work was done by Michael Pelletier of Caltech for NASA's Jet Propulsion Laboratory. Further information is contained in a TSP (see page 1).

In accordance with Public Law 96-517, the contractor has elected to retain title to this invention. Inquiries concerning rights for its commercial use should be addressed to

Intellectual Assets Office

JPL

Mail Stop 202-233

4800 Oak Grove Drive

Pasadena, CA 91109-8099

(818) 354-2240

E-mail: ipgroup@jpl.nasa.gov

Refer to NPO-30711, volume and number of this NASA Tech Briefs issue, and the page number.



Adaptation of Mesoscale Weather Models to Local Forecasting

Both objective and subjective evaluation methodologies are needed.

John F. Kennedy Space Center, Florida

Methodologies have been developed for (1) configuring mesoscale numerical weather-prediction models for execution on high-performance computer workstations to make short-range weather forecasts for the vicinity of the Kennedy Space Center (KSC) and the Cape Canaveral Air Force Station (CCAFS) and (2) evaluating the performances of the models as configured. These methodologies have been implemented as part of a continuing effort to improve weather forecasting in support of operations of the U.S. space program. The models, methodologies, and results of the evaluations also have potential value for commercial users who could benefit from tailoring their operations and/or marketing strategies based on accurate predictions of local weather.

More specifically, the purpose of developing the methodologies for configuring the models to run on computers at KSC and CCAFS is to provide accurate forecasts of winds, temperature, and such specific thunderstorm-related phenomena as lightning and precipitation. The purpose of developing the evaluation methodologies is to maximize the utility of the models by providing users

with assessments of the capabilities and limitations of the models.

The models used in this effort thus far include the Mesoscale Atmospheric Simulation System (MASS), the Regional Atmospheric Modeling System (RAMS), and the National Centers for Environmental Prediction Eta Model ("Eta" for short). The configuration of the MASS and RAMS is designed to run the models at very high spatial resolution and incorporate local data to resolve fine-scale weather features. Model preprocessors were modified to incorporate surface, ship, buoy, and rawinsonde data as well as data from local wind towers, wind profilers, and conventional or Doppler radars.

The overall evaluation of the MASS, Eta, and RAMS was designed to assess the utility of these mesoscale models for satisfying the weather-forecasting needs of the U.S. space program. The evaluation methodology includes objective and subjective verification methodologies. Objective (e.g., statistical) verification of point forecasts is a stringent measure of model performance, but when used alone, it is not usually sufficient for quantifying the value of the overall contribu-

tion of the model to the weather-forecasting process. This is especially true for mesoscale models with enhanced spatial and temporal resolution that may be capable of predicting meteorologically consistent, though not necessarily accurate, fine-scale weather phenomena. Therefore, subjective (phenomenological) evaluation, focusing on selected case studies and specific weather features, such as sea breezes and precipitation, has been performed to help quantify the added value that cannot be inferred solely from objective evaluation.

This work was done by John T. Manobianco, Gregory E. Taylor, Jonathan L. Case, Allan V. Dianic, and Mark W. Wheeler of ENSCO, Inc., John W. Zack of MESO, Inc., and Paul A. Nutter formerly of ENSCO, Inc., for Kennedy Space Center. For further information, contact John Manobianco at (321) 853-8202 or via e-mail at manobianco.john@ensco.com or refer to "Evaluation of the 29-km Eta Model. Part I: Objective Verification at Three Selected Stations" and "Evaluation of the 29-km Eta Model. Part II: Subjective Verification over Florida" in Weather and Forecasting, Volume 14 (February 1999), published by the American Meteorological Society. KSC-12241

Aerodynamic Design Using Neural Networks

The amount of computation needed to optimize a design is reduced.

Ames Research Center, Moffett Field, California

The design of aerodynamic components of aircraft, such as wings or engines, involves a process of obtaining the most optimal component shape that can deliver the desired level of component performance, subject to various constraints, e.g., total weight or cost, that the component must satisfy. Aerodynamic design can thus be formulated as an optimization problem that involves the minimization of an objective function subject to constraints.

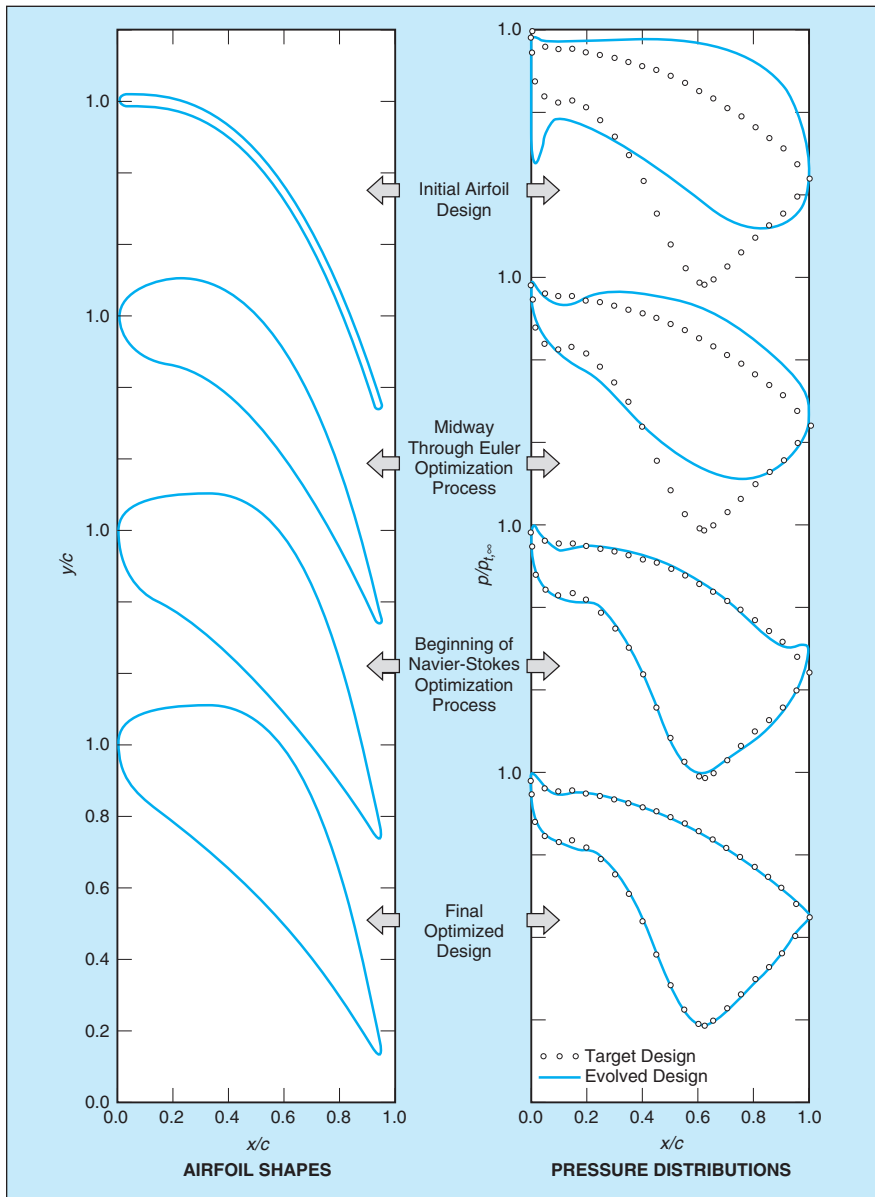
A new aerodynamic design optimization procedure based on neural networks

and response surface methodology (RSM) incorporates the advantages of both traditional RSM and neural networks. The procedure uses a strategy, denoted parameter-based partitioning of the design space, to construct a sequence of response surfaces based on both neural networks and polynomial fits to traverse the design space in search of the optimal solution.

Some desirable characteristics of the new design optimization procedure include the ability to handle a variety of design objectives, easily impose constraints, and incorporate design guidelines and

rules of thumb. It provides an infrastructure for variable fidelity analysis and reduces the cost of computation by using less-expensive, lower fidelity simulations in the early stages of the design evolution. The initial or starting design can be far from optimal. The procedure is easy and economical to use in large-dimensional design space and can be used to perform design tradeoff studies rapidly. Designs involving multiple disciplines can also be optimized.

Some practical applications of the design procedure that have demonstrated



The **Design Procedure** can evolve a generic shape into an optimized airfoil that matches a target pressure distribution. Position coordinates (x and y) are normalized to the chord length (c); local pressure (p) is normalized to the turbine inlet total pressure ($p_{t, \infty}$).

some of its capabilities include the inverse design of an optimal turbine airfoil starting from a generic shape and the redesign of transonic turbines to improve their unsteady aerodynamic characteristics.

In one practical application, the procedure was used to reconstruct the shape of a turbine airfoil given a desired pressure distribution and some relevant flow and geometry parameters. The shape of the airfoil was not known beforehand. Instead, it was evolved from a simple curved section of nearly uniform thickness. The evolved optimal airfoil closely matched the shape of the original airfoil that was used to obtain the pressure distribution. The progression of the design is depicted in the figure. The airfoil shape evolution is shown on the left, while the corresponding pressure distributions and the target pressure distribution are shown on the right. The surface pressures approach the target distribution as the design progresses until the optimal airfoil shown at the bottom has a pressure distribution that matches closely the target.

The technology developed and implemented in the neural-network-based design optimization procedure offers a unique capability that can be used in other aerospace applications such as external aerodynamics and multidisciplinary optimization, and has potential applications beyond aerospace design.

This work was done by Man Mohan Rai and Nateri K. Madavan of Ames Research Center. Further information is contained in a TSP (see page 1).

This invention is owned by NASA, and a patent application has been filed. Inquiries concerning nonexclusive or exclusive license for its commercial development should be addressed to the Patent Counsel, Ames Research Center, (650) 604-5104. Refer to ARC-14281.

Combining Multiple Gyroscope Outputs for Increased Accuracy

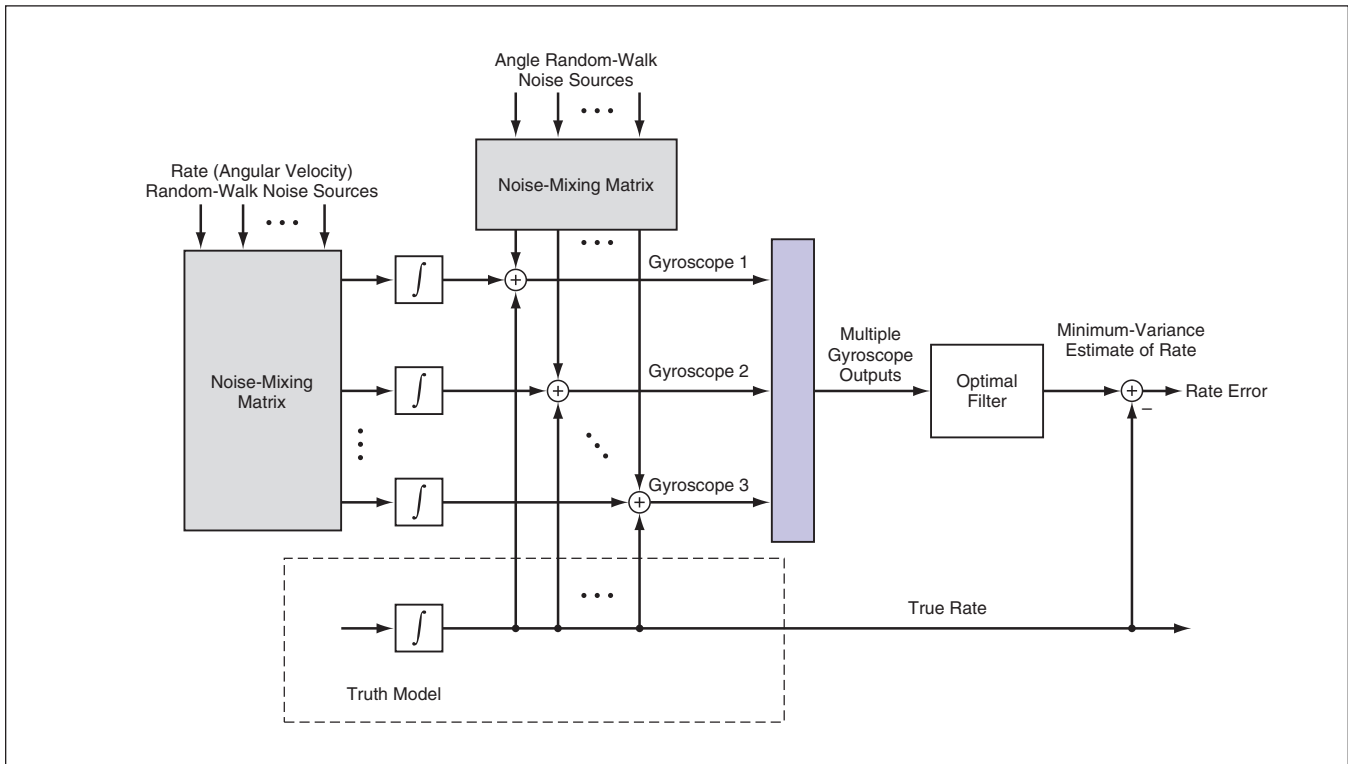
A lightweight, low-power, compact MEMS gyroscope array could perform comparably to a larger more-conventional gyroscope.

NASA's Jet Propulsion Laboratory, Pasadena, California

A proposed method of processing the outputs of multiple gyroscopes to increase the accuracy of rate (that is, angular-velocity) readings has been developed theoretically and demonstrated by computer simulation. Although the method is applicable, in principle, to any gyroscopes, it is intended especially for application to gy-

roscopes that are parts of microelectromechanical systems (MEMS). The method is based on the concept that the collective performance of multiple, relatively inexpensive, nominally identical devices can be better than that of one of the devices considered by itself. The method would make it possible to synthesize the readings of a single,

more accurate gyroscope (a "virtual gyroscope") from the outputs of a large number of microscopic gyroscopes fabricated together on a single MEMS chip. The big advantage would be that the combination of the MEMS gyroscope array and the processing circuitry needed to implement the method would be smaller, lighter in



Readings From Multiple Gyroscopes would be combined by use of an optimal (minimum-variance) filter, thereby synthesizing the readings of what amounts to a more accurate virtual gyroscope.

weight, and less power-hungry, relative to a conventional gyroscope of equal accuracy.

The method (see figure) is one of combining and filtering the digitized outputs of multiple gyroscopes to obtain minimum-variance estimates of rate. In the combining-and-filtering operations, measurement data from the gyroscopes would be weighted and smoothed with respect to each other according to the gain matrix of a minimum-variance filter. According to Kalman-filter theory, the gain matrix of the minimum-variance filter is uniquely specified by the filter covariance, which propagates according to a matrix Riccati equation. The present method incorporates an exact analytical solution of this equation.

The analytical solution reveals a wealth of theoretical properties and enables the consideration of several practical implementations. Among the most notable theoretical properties are the following:

- Even though the terms of the Riccati equation grow in an unbounded fashion, the Kalman gain can be shown to approach a steady-state matrix. This result is fortuitous because it simplifies implementation and can serve as a basis of practical schemes for realizing the optimal filter by use of a constant-gain matrix.

- The analytical solution enables the development of a complete statistical theory that characterizes the drift of the virtual gyroscope and provides theoretical limits of improvement obtainable by use of an ensemble of correlated sensors as a single virtual sensor.
- The minimum-variance gain matrix has been analyzed in detail. The structure of the gain matrix indicates the presence of a marginally unstable pole, which would make implementation impossible if it were not properly understood and compensated. In addition, a simple algebraic method for computing the optimal gain matrix has been developed, making it possible to avoid the Riccati equation completely.
- The notion of statistical common-mode rejection (CMR) has been characterized mathematically. For statistically uncorrelated gyroscopes, it is shown that the component drift variances add like parallel resistors (e.g., in units of $\text{rad}^2/\text{sec}^3$). For identical devices, this means that the combined drift is reduced by a factor of $1/\sqrt{N}$ compared to the individual gyroscope drift, where N is the number of gyroscopes being combined.
- Potential improvement in drift is much more impressive when the de-

vices are correlated. For correlated gyroscopes, an exact mathematical expression is developed for the combined drift. The expression indicates that the internal noise sources count to the extent that they infect multiple devices coherently (e.g., with common sign), and can be removed to the extent that they infect multiple devices incoherently (e.g., with randomized signs). Noise eliminated by correlations between devices can potentially reduce the virtual gyroscope drift far beyond the $1/\sqrt{N}$ factor attainable using uncorrelated devices.

This work was done by David S. Bayard of Caltech for NASA's Jet Propulsion Laboratory. Further information is contained in a TSP (see page 1).

In accordance with Public Law 96-517, the contractor has elected to retain title to this invention. Inquiries concerning rights for its commercial use should be addressed to

Intellectual Assets Office

JPL

Mail Stop 202-233

4800 Oak Grove Drive

Pasadena, CA 91109

(818) 354-2240

E-mail: ipggroup@jpl.nasa.gov

Refer to NPO-30533, volume and number of this NASA Tech Briefs issue, and the page number.

Improved Collision-Detection Method for Robotic Manipulator

Collisions are detected in a computationally efficient manner.

NASA's Jet Propulsion Laboratory, Pasadena, California

An improved method has been devised for the computational prediction of a collision between (1) a robotic manipulator and (2) another part of the robot or an external object in the vicinity of the robot. The method is intended to be used to test commanded manipulator trajectories in advance so that execution of the commands can be stopped before damage is done. The method involves utilization of both (1) mathematical models of the robot and its environment constructed manually prior to operation and (2) similar models constructed automatically from sensory data acquired during operation. The representation of objects in this method is simpler and more efficient (with respect to both computation time and computer memory), relative to the representations used in most prior methods.

The present method was developed especially for use on a robotic land vehicle (rover) equipped with a manipulator arm and a vision system that includes stereoscopic electronic cameras. In this method, objects are represented and collisions detected by use of a previously developed technique known in the art as the method of oriented bounding boxes (OBBs). As the name of this technique indicates, an object is represented approximately, for computational purposes, by a box that encloses its outer boundary. Because many parts of a robotic manipulator are cylindrical, the OBB method has been extended in this

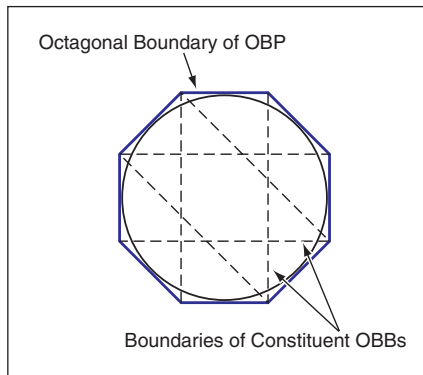


Figure 1. A Rodlike Robot Arm of Circular Cross Section, viewed here along its axis, can be represented by an octagonal OBP assembled from four smaller OBBs.

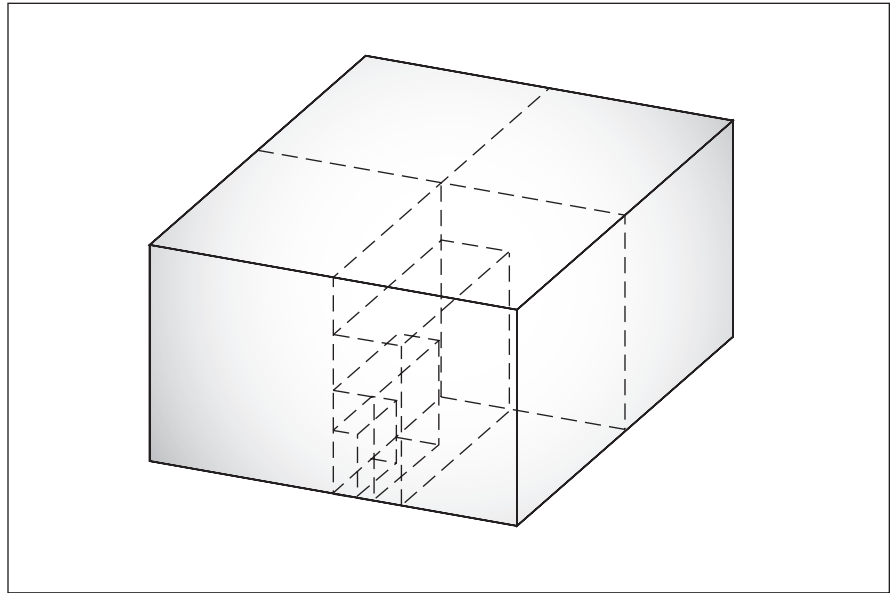


Figure 2. A Hierarchy of OBBs of successively finer resolution is used to represent terrain elevation as a function of horizontal coordinates.

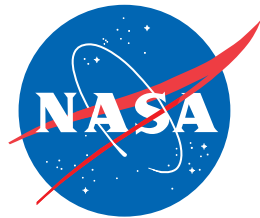
method to enable the approximate representation of cylindrical parts by use of octagonal or other multiple-OBB assemblies denoted oriented bounding prisms (OBPs), as in the example of Figure 1. Unlike prior methods, the OBB/OBP method does not require any divisions or transcendental functions; this feature leads to greater robustness and numerical accuracy. The OBB/OBP method was selected for incorporation into the present method because it offers the best compromise between accuracy on the one hand and computational efficiency (and thus computational speed) on the other hand.

OBBs are also used to represent the terrain and any objects on the terrain sensed by the stereoscopic vision system. A conceptual multiresolution map pyramid of the manipulator work space is computed from the stereoscopic sensory data and is then used in a coarse-to-fine sequence to detect collisions between the manipulator and terrain. As described next, tests for collisions are performed in a hierarchical sequence to minimize the amount of computation needed to detect collisions.

Starting with the second-highest level of the pyramid, each level is characterized by

twice the horizontal spatial resolution of the level above it (see Figure 2). For example, at the highest level of the pyramid (coarsest resolution) there is a single terrain OBB that encloses all of the sensed data points. The model for each manipulator link is one low-resolution OBP. If no collisions between any of the OBPs and the coarsest-resolution terrain OBB are detected, then there is no need for further computation to detect collisions with terrain. On the other hand, if collisions are detected at the coarsest resolution, then tests for collisions are performed on each of the terrain OBBs at the second coarsest resolution. This process continues to successively finer levels of resolution until the finest resolution is reached or no more collisions are detected. Similar tests for collisions are performed with a similarly hierarchical model of the non-manipulator parts of the robot (body, cameras, sensors, suspension, and wheels).

*This work was done by Chris Leger of Caltech for NASA's Jet Propulsion Laboratory. Further information is contained in a TSP (see page 1).
NPO-30356*



National Aeronautics and
Space Administration